

See discussions, stats, and author profiles for this publication at: <https://www.researchgate.net/publication/319354915>

Platinum–group elements (PGE), Re, Ni, Cu, Ag and Cd variations along the Reykjanes Ridge and Iceland South–West...

Working Paper · August 2017

DOI: 10.1594/IEDA/100712

CITATIONS

0

2 authors, including:



Jean-Guy Schilling

University of Rhode Island

188 PUBLICATIONS 11,334 CITATIONS

SEE PROFILE

Some of the authors of this publication are also working on these related projects:



Mantle plume ridge interactions [View project](#)

Platinum-group elements (PGE), Re, Ni, Cu, Ag and Cd variations along the Reykjanes Ridge and Iceland South-West Neovolcanic Rift Zone, from 50°N to 65°N: Implications on sulfide bearing PGE mantle source heterogeneities and partial melting effects.

Jean-Guy Schilling*, *Graduate School of Oceanography, University of Rhode Island, Kingston, RI, 02881, USA (jgs@gso.uri.edu)*

Richard H. Kingsley, *Graduate School of Oceanography, University of Rhode Island, Kingston, RI, 02881, USA (kingsley@gso.uri.edu)*

** Corresponding Author*

Current address: P.O. Box 77, Jamestown, RI 02835, U.S.A.

Unpublished working paper accompanying data sets DOI:10.1594/IEDA/100712

Abstract

We report on platinum group elements (PGE), Re, Ni, Cu, Ag and Cd concentrations of 53 tholeiitic basalts and one picrite from the Reykjanes Ridge and its extension over Iceland. We emphasize that our interpretation of these data is based primarily on the along-ridge spatial variations, considering that the nature of the large-scale sampling and sampling-intervals involved preclude determining local consanguineous basaltic melt evolutions. The concentration of PGE, Cu and Ag show a strong progressive northward increase toward Iceland, which are uncorrelated with that of MgO, Ni and Cr. The latter show a minimum around 63.5°N, due to enhanced silicate fractional crystallization, mostly without significant sulfide removal. At MgO contents of 7-9%, the Iceland basalts relative to the 50-54°N N-MORB unaffected by the Iceland mantle plume are systematically enriched by a factor ~10 and ~15 in Pd and Ir, respectively. Sulfur, Cu and Pd variations show that the 50-54°N N-MORB and T-MORB are sulfide saturated, whereas the Iceland basalts are sulfide-unsaturated, but sulfur-vapor/melt saturated. Other PGE show intermediate enrichments between Pd and Ir. Cu is enriched by a factor of 2. Re also increases northward up to 63.5°N until it drops drastically over Iceland due in part to volatile degassing and retention by residual garnet upon melting. The high-P garnet melting effect over Iceland is corroborated by the accompanying drop of SiO₂ and Yb over Iceland, the HREE cross-over patterns, and Pd/Ir ratio variations along the profile. Cd shows a mixed behavior between Re and Cu. Cu and Ag latitudinal variations are very similar, resulting in an essentially constant Cu/Ag ratio of 3292 +/- 704 std. Two distinct models, not necessarily mutually exclusive were considered: 1) Two mantle sources distinct in Pd and Ir contents and their mixing along the ridge, as previously evident from Pb-Nd-Sr-He isotope and (La/Sm)_n variations of the same samples. 2) Possibly, increasing partial melting towards Iceland of a uniform sulfide-bearing primary mantle source (PUM) with PGE content hosted entirely in the sulfide. We show that the extremely low PGE contents of the 50-54°N N-MORB, unaffected by the Iceland mantle plume, cannot be accounted for by such a melting model, even with using the higher $K^{\text{sulfide melt/silicate melt}}$ of 1×10^5 and 1×10^6 for Pd and Ir recently reported by Mungall and Brenan (2014), compared to $\sim 1-5 \times 10^4$ previously considered (e.g. Peach et al., 1994; Rehkämper et al. 1999b; Bézou et al., 2005). The extent of the PGE, Cu, Ag, Re and Cd depletion in the Depleted MORB Mantle (DMM) relative to the Iceland mantle plume source remains model dependent, and cannot be quantified at this point. We also show that fractional crystallization of

silicates involving PGE-rich immiscible sulfides has limited effects on the PGE, Cu, Ag, Re and Cd large-scale gradients observed along the Reykjanes Ridge, with the exception of Ru that shows very large overall scatter.

1. Introduction

It is now well established that the PGE budget of fertile peridotites with essentially chondritic PGE relative abundances is dominated by intergranular sulfides (e.g. Jagoutz et al 1979, Mitchell and Keays 1981; Hart and Ravizza 1996; Guo et al., 1999; Lorand and Alard 2001; Pearson et al., 2004). Upon partial melting of such rocks, the PGE contents and their relative abundances in generated silicate melts are also dominantly controlled by residual sulfides. Their very high $K^{\text{sulfide melt / silicate melt}}$ partition coefficients, usually assumed of the order of 10^4 - 10^5 , are likely to lead to extremely low PGE concentrations in basaltic melts, and their relative fractionation as a function of the degree of partial melting (e.g. Fryer and Greenough 1992; Keays 1995; Rehkämper et al., 1997, Momme et al., 2003, and references there in). Moreover, $K^{\text{sulfide melt / silicate melt}}$ the order of 10^5 - 10^6 have also recently been reported by Mungall and Brenan (2014).

The high and essentially chondritic PGE relative abundances of fertile peridotite xenoliths found by Jagoutz et al., (1979), Morgan (1981 and 1986), have led support to the heterogeneous accretion model for the Earth initially proposed by Turekian and Clarke (1969) and Chou et al. (1983). The model assumes first segregation of the iron core, followed by a small late veneer addition of chondritic material and re-homogenization of the mantle by convection.

However, more recently, non-chondritic relative PGE abundances in abyssal peridotites (Rehkämper et al., 1997, Luguet et al. 2001, 2003) and orogenic peridotites (Pattou et al., 1996; Lorand et al., 1999) have revealed both small-scale and large-scale PGE mantle heterogeneities. The cause of such fractionation is still being debated. It has been suggested that the supra-chondritic Pd/Ir ratio of oceanic peridotites may be due to addition of sulfides by percolating melts into the depleted residue of melting (Rehkämper et al., 1997, Lorand et al. 2008, Luguet et al. 2001, 2003). This has also been attributed to small inputs of differentiated outer-core bleb material into the lower mantle (Snow and Schmidt, 1998), and transported by mantle plumes derived from the core/mantle boundary (e.g. Fryer and Greenough, 1992; Brandon et al., 1998).

PGE evidences from MORB and OIB, the complements of residual mantle peridotites, have been lagging far behind because of their very low abundances, analytical limitations in measurement and detection, until the advent of inductively coupled mass spectrometry ICP-MS, and with isotopic dilution (ID-ICPMS). So far the few PGE data reported in basalts suggest that the mantle source from hotspots may be PGE richer than the source of normal mid-ocean ridge basalts (N-MORB). These include Reunion (Fryer and Greenough 1992), Hawaii (Tatsumi et al., 1999, Bennett et al., 2000 and Crocket, 2000), Cook islands (Tatsumi et al., 2000), and the Ontong Java Plateau (Ely and Neal 2003). Could Iceland be another case?

To further evaluate this question, we now report on PGE, Re, Ni, Cu, Ag and Cd, spatial variations in basalts along the Reykjanes Ridge and its extension over the Iceland SW Neovolcanic Zone (SWNZ), from 50°N to 65°N (Fig. 1). Numerous Sr, Pb, Nd, Hf and He isotope ratio variations (e.g. Fig 2), trace element and petrologic studies of these very same basalts have shown that this region of the Mid-Atlantic Ridge is the locus of a dynamical mixing interaction and dilution of the Iceland mantle plume with DMM, also called the depleted upper mantle (DMU) (Blichert-Toft et al., 2005; Hart et al., 1973; Poreda et al., 1986; Schilling, 1973; Schilling et al., 1983; Sun et al., 1975)

Our interpretation will emphasize primarily the relative spatial variations observed. This is only permitted considering the nature of our overall large-scale sampling (~1665 km) and interval-scale (~31 km on average). None of these samples are likely to be consanguineous and adequate in revealing directly local effects, such as fractional crystallization. However, the region should potentially help distinguishing between 1) two distinct mantle sources in PGE contents, and/or 2) PGE variations resulting simply from increasing degree of melting toward the Iceland hotspot, as considered in the thermal and dynamical plume models of (White et al., 1995; Ito et al., 1996 and 1999).

2. Sample Background

The location along the ridge axis of the 54 basalts analyzed for PGE, Re, Ni, Cu, Ag and Cd are shown in Fig.1, and their dredging elevations in Fig. 2. Samples shown in red are light-REE enriched from the Iceland SWNZ with chondrite-normalized $(La/Sm)_n > 1$. Those in blue are

light-REE depleted with $(La/Sm)_n < 0.5$, which are referred as normal MORB (N-MORB) (Schilling et al. 1983). The green samples are intermediate and reflect the mixing zone initially discovered by Schilling (1973). They are referred as transitional MORB (T-MORB).

The petrologic characteristics of these basalts have been studied in detail. They are all olivine to slightly quartz normative tholeiitic basalts, with the exception for one strongly light-rare earth (REE) depleted sub-glacial erupted glassy picrite (Ic117g). Whole-rock major, REE and other trace element contents, as well as phenocryst modal abundances, and their petrographic assemblages (including % vesicles), can be found in Schilling et al. (1983), and Moore and Schilling (1973). Major elements of the glass rims of these MORB and the sub-glacial Iceland basalts can be found in Sigurdsson (1981), and 40 trace elements from the Reykjanes Ridge basalt glasses in Kelley et al. (2013).

Noteworthy for subsequent interpretation is the pronounced minimum in Mg-value (i.e., molar $Mg/[Mg+Fe]$; or MgO) and Ni content observed around 63.5°N (Fig. 3.1 and 3.3). This minimum also corresponds to a minimum in the temperature of crystallization of olivine micro-phenocrysts present in these basalts (Hermes and Schilling, 1976; Schilling and Sigurdsson, 1979), which has been confirmed by melting and re-crystallization experiments (Fisk, 1978; Fisk et al., 1980). The paragenetic sequence of crystallization of olivine, plagioclase and clinopyroxene observed in these melting experiments suggests crystallization within a pressure range of 0.2-0.62 GPa, with a minimum coinciding with the minimum-T and maximum extent of crystallization observed along the Reykjanes Ridge. The more extensive low-P crystallization in this region coincides with the thicker crust of the Iceland shelf margin and the small en-echelon shifts of the ridge axis as it approaches the leaky transform fault zone present over the Reykjanes Peninsula and eastward.

3. Analytical Methods

Ir, Ru, Pt, Pd, Ag, Cd and Re concentrations were obtained by isotopic dilution (ID) analyses with a high-resolution inductively coupled mass spectrometer (HR-ICP-MS, Finnigan ELEMENT). The method was adapted from that of Pearson and Woodland (2000) with attention to minimizing blank levels and interfering masses during ICPMS analyses. The schematic flow

chart of the method is shown in Appendix A, Fig. A1a. One to three grams of cleaned glass or interior rock chips were weighed into screw-top Teflon beakers (Savillex) and dissolved in hydrofluoric and nitric acid. Prior to dissolution, the samples were spiked with a solution of Oak Ridge enriched isotopes. These were ^{99}Ru , ^{105}Pd , ^{106}Cd , ^{109}Ag , ^{185}Re , ^{191}Ir and ^{198}Pt . The sample/spike mixture was dried, converted to chlorides and oxidized. Separation of the PGE, Ag, and Cd from the rock matrix was performed using an anion exchange column (1x8, 100-200 mesh, elution curve available on request). The isotope ratios measured in the HR-ICP/MS analytical step were $^{99}\text{Ru}/^{101}\text{Ru}$, $^{105}\text{Pd}/^{108}\text{Pd}$, $^{185}\text{Re}/^{187}\text{Re}$, $^{191}\text{Ir}/^{193}\text{Ir}$, $^{198}\text{Pt}/^{195}\text{Pt}$, $^{109}\text{Ag}/^{107}\text{Ag}$ and $^{106}\text{Cd}/^{111}\text{Cd}$. Analytical precision was determined from our in-house mid-ocean ridge basalt standard (EN026 10D-3). Table A1 in Appendix A reports these results, with precision, and blank levels for 1-3g replicate samples. Unfortunately, no “certified” PGE sub-nanogram/g level basalt standards were available for testing the accuracy of our laboratory ID-HR-ICPMS method for MORB glasses. To overcome this limitation we initiated an inter-laboratory comparison of our in-house basalt standard EN026 10D-3 with other laboratories (Kingsley et al., 2004). Results of this exchange are displayed in Appendix A, Fig. A2, and Table A2. Appendix A, Table A3 also compares our results for standards BIR-1 picrite and BHVO-1 basalt with values reported by Govindaraju (1994), all of which are characterized as “informational values” due to the difficulty of measuring low levels of the PGE in these basalt standards. The comparisons are satisfactory considering the very low-level of PGE in MORB and the possible PGE sample heterogeneities in prepared rock standards caused by the so-called “micro-nugget effect”, referring to highly dispersed micro PGE -metal alloys (PGM) possibly present, but undetectable.

Os concentrations were determined independently from the other PGE, using about 2 gm of basalt. It was analyzed by ID-HR-ICP-MS, following a procedure modified from Hassler et al., (2000), but using a high temperature and pressure microwave Hydrofluoric and Nitric Acid dissolution, which avoids the relatively high blank problems with fusion, Parr bomb, and NiS assay methods usually used by other laboratories. The microwaved solutions were then sparged (argon gas carries OsO_4) into the URI high resolution and sensitivity magnetic sector ICP-MS (Thermo-Finnigan ELEMENT) to measure the $^{190}\text{Os}/^{192}\text{Os}$ ratio, with ^{190}Os being the enriched spike. The schematic flow chart of the method is shown in Appendix FigA1b.

The procedure blank for Os was determined by treating pure silica powder as a sample. This provided a procedure blank value of 69 ± 20 picograms of Os per analysis, which was subtracted from all the MORB analyses. This was generally less than 3% of the measured Os, but in some very low-level samples, the correction was significant (up to 13%).

The precision of the Os method was determined by analyzing both the glass portion and the interior crystalline portion of our in-house MORB standard EN026 10D-3 (Mohns Ridge MORB). The result of 19 analyses was 0.014 ± 0.002 (1s) ng/g. The accuracy is estimated by comparing this value to those obtained by other PGE analytical laboratories where this standard was also analyzed by various methods. The comparison with our method is excellent (Appendix Table A2).

Ni and Cu concentrations were obtained by a routine external and internal standardization HR-ICP-MS method at URI (Schilling et al. 1999). Precision and accuracy of these 2 elements based on our in-house MORB standard EN026 10D-3 (n=42) was 3.4% for Ni and 4.0% for Cu. The accuracy for the analyses of these two elements was good and is established by comparison with certified USGS standards BHVO-1 and BCR-1 in Appendix A, Table 4.

4. Results.

Table 1 lists the PGE, Re, Ag and Cd concentrations in ppb, and the Ni and Cu concentrations in ppm, for the 54 basalts analyzed in this study. Included for reference are the MgO concentrations and the chondrite-normalized (La/Sm)_n ratios of these basalts.

5. Latitudinal Variations

5.1 PGE.

The along-ridge PGE basalt spatial variations from 50°N to 65°N are shown in Fig. 3.1 and 3.2. The PGE show on a logarithmic scale a progressive increase from the Gibbs fracture zone, where light-REE depleted N-MORB are present, toward and over the Iceland Southwest Neovolcanic Zone (SWNZ) characterized by light-REE enriched patterns (Schilling, 1973). The trends are similar to that of Sr, Pb, Nd, Hf and He isotope ratios, suggesting the possibility of two mantle sources with distinct PGE content and their mixing along the ridge (e.g. Fig. 2). The PGE gradients are most pronounced for Pd, Ir while Pt, Os and Ru are more subdued and show larger local scatter. The high PGE values are found over Iceland SWNZ, particularly for Pd and Ir.

They are comparable in range with other Iceland tholeiitic basalts reported by Momme et al. (2003) and Rehkämper et al. (1999b) over the same 6-11 % MgO range of our samples. They are also comparable to tholeiites from the Reunion hotspot (Fryer and Greenough, 1992] and Hawaii hotspot (Tatsumi et al., 1999; Bennett et al. 2000 ; Crocket, 2000).

The lowest PGE contents are found on the Reykjanes Ridge south of 60°N, along the so-called N-MORB segment with $(La/Sm)_n < 0.5$ (Schilling et al., 1983). These basalts are comparable and even lower in PGE content than other MORB so far reported from the Atlantic and Indian Oceans (Hertogen et al., 1980; Fryer and Greenough, 1992; Rehkämper et al., 1999; Tatsumi et al., 1999, Bézos et al., 2005), with the exception of the very low PGE MORB content from the ~ 15°S East Pacific Rise reported by Rehkämper et al. [1999b].

Basalt averages from the Iceland SWNZ relative to that of the 50-54°N N-MORB group indicate enrichment factors (EF) of 76, 40 and 11, for Pd, Ir and Pt, respectively; and only about 9 for Ru and Os.

5.2. *Cu and Ag.*

Cu shows also a progressive increase from 50°N toward and over the Iceland SWNZ, on a linear scale, which is uncorrelated with that of Ni (Fig 3.3). Ag latitudinal variation is very similar to that of Cu resulting in an essentially constant Cu/Ag ratio of 3292 +/- 704 sd.

5.3. *Ni, Cr and MgO.*

In contrast, as indicated earlier, MgO as well as Ni and Cr show a pronounced minimum around 63°N (Figs. 3.1 and 3.3) The along-ridge minimum corresponds to a maximum of some 50-60% crystallization and removal of a mixture of olivine-plagioclase-pyroxene in proportions of about 1:3:2 prior to eruption (Hermes and Schilling, 1976). Any fractionation involving sulfides would be readily noticeable considering that the PGE partition coefficients, $K^{\text{sulfide/silicate melt}}$ are of the order of 10^4 - 10^6 , whereas $K^{\text{silicate crystal/silicate melt}}$ are close to zero (e.g Peach et al. 1990 and 1994, Bézos et al. 2005, Mungall and Brenan 2014).

The minimum in Mg-value, Ni (and Cr not shown) does not appear to have any significant effect on that of the PGE spatial trend observed (compare Fig 3.1, 3.2 and 3.3), indicating that late stage-silicate fractional crystallization is not a major factor in controlling the large scale PGE

variations along the ridge, nor does it involve any significant PGE-rich sulfide and/or PGE alloys removal.

Overall, the maximum 50-60% low-P, late-stage silicate fractional crystallization effect around 63.5°N is mostly limited in PGE removal. The above observations suggest the Iceland mantle plume is enriched in PGE and Cu relative to the surrounding DMM, as also suggested for other hotspots, such as the Reunion hotspot (Fryer and Greenough, 1992), Hawaii (Tatsumi et al., 1999; Bennett et al., 2000; Crocket, 2000) and the Cook islands (Tatsumi et al., 2000). This conclusion is further supported in Section 7.

5.4. *Re and Cd*

Re concentration also increases by a factor of ~ 2 northward up to 63.5°N, until it drops drastically over Iceland, as does SiO₂, Yb, and Cd (Fig. 4). The drop in Re is apparently related in part to volatile degassing and/or retention by residual garnet upon melting (Lassiter, 2003, Bennett et al., 2000, Hauri and Hart, 1997). Cd shows a mixed behavior between Re and Cu. Re contents lower than MORB have also been observed in alkali ocean island basalts, which may be related to the compatibility of Re in garnet and/or sulfides (Hauri and Hart, 1997).

1) On one hand, in the absence of residual sulfides during melting, this drop over Iceland may be attributed to the compatibility of Re in garnet ($K_{\text{garnet/melt}} \sim 2.7$) and its retention in garnet-bearing mantle residue during high pressure partial melting, as for the heavy RE such as Yb ($K_{\text{garnet/melt}} 2-8.7$) (Righter and Hauri, 1998). The lower SiO₂ and Yb over the Iceland SWNV zone, and HREE cross-over patterns for basalts from of Iceland relative to Reykjanes Ridge N-MORB would appear consistent with this idea (Schilling et al., 1983). The question can be further evaluated by examining the spatial variation of Re/Yb along the MAR, which is dominated by the Re variation (Fig.5a). Lower Re and Re/Yb over Iceland might be explained if more residual sulfide phases were present during partial melting of the Iceland plume relative to the N-MORB source because of the relatively high $K_{\text{sulfide/silicate melt}}$ partition coefficients for Re (~ 43 (Roy-Barman et al., 1998) to 1200 (Jones and Drake, 1986).

However, the PGE variation is much more sensitive to sulfide/silicate fractionation effects because of their much higher $K_{\text{sulfide/silicate melt}}$ than Re which suggests the converse! In fact, Re/PGE ratios stay fairly constant along the Reykjanes Ridge as both PGE and Re increase, but then the ratio drops over Iceland due to the lowering of the Re content while the PGE keep

increasing, such as Re/Ir shown in Fig 5b). A key question to be resolved is why Re over Iceland is depleted yet the PGE are enriched (compare Figs. 3 and 4)

2) An alternate hypothesis is that the low Re over Iceland may be due to some Re loss upon subaerial eruption and degassing due to its volatility. This is supported by the low Re abundances in subaerial versus submarine basalts erupted in the HSDP-2 Mauna Kea Drillcore in Hawaii (Lassiter 2003), as well as the high Cu/Re ratios of some basalts from Hawaii (Bennett et al., 2000). Cl and Cu/Re variations along the Iceland-Reykjanes Ridge profile from the same basalts corroborate these two models (Fig.5c and 5d). On one hand, low pressure (<500m water depth) T-MORB erupting on the northern part of the Reykjanes Ridge over the insular Iceland platform, which on the basis of Cl, water and S are partly degassed (Fig.2 and 5c), have similar Cu/Re ratios to non-degassed N-MORB located further south, whereas basalts over Iceland have clearly high Cu/Re ratios (Fig.5c), due to the high Cu and low Re contents (Fig.3.3 and 4, respectively). Furthermore, at shallower than 500 m water depth of eruption, T-MORB and the Iceland subaerial-erupted basalt population shows a good positive correlation between Re and melt-retained Cl, (Fig 6a&b), as well as an inverse correlation of Cu/Re with melt-retained Cl (Fig.6c), thus supporting Re outgassing!

Quantitative evaluation of the relative extent of the garnet and degassing effects on Re variation is beyond the scope of this paper.

6. PGE Fractionation Patterns

The primitive-mantle-normalized PGE fractionation patterns are shown in Fig. 7. The patterns of the SWNZ Iceland basalts (with $(La/Sm)_n > 1$) are mostly higher than the N-MORB (i.e. $0.22 < (La/Sm)_n < 0.66$). Yet, the two groups have a similar degree of PGE fractionation, with overlapping primitive mantle normalized $(Pd/Ir)_n$ ratios in the range of 29-119 for Iceland basalts and 14-187 for N-MORB. T-MORB from the mixing zone (with $0.17 < (La/Sm)_n < 1.27$) have intermediate PGE enrichment patterns but more fractionated and variable with $(Pd/Ir)_n$ in the range of 25-278 around 63.5°N, where the MgO, Ni and olivine crystallization T- minimum occurs. Again as anticipated, these observations suggest that the PGE pattern variations are not merely the result of a two-mantle source mixing. In quantitative term, the patterns neither readily resolve the extent by which the observed PGE variations along the ridge have been affected by

fractional crystallization, partial melting or distinct mantle source heterogeneities. Their detailed internal PGE fractionation is not discussed in this paper.

7. Fractional crystallization at the 63.5°N Mg-value minimum.

This minimum in magma temperatures and maximum extent of low-P crystallization is dominated by removal of a mixture of olivine-plagioclase-pyroxene in proportions of about 1:3:2 (Hermes and Schilling, 1976). Relative to the large-scale PGE spatial trend, somewhat lower PGE values are noticeable over this region, which are most pronounced for Ir and Ru (Fig. 3.2). In contrast, Cu is slightly enhanced in this region (Fig. 3.3), resulting in a well-defined dip in the Ni/Cu ratio in the 63.5°N region (not shown). This minimum suggests a combined silicate fractional crystallization effect, accompanied by some minor sulfide and/or PGE-alloy removal. It is also supported from the observation that most PGE (as well as Cu) are essentially incompatible in silicates minerals (i.e. silicate crystal/melt partition coefficients < 1), with the possible exception of olivine and spinel, but which also may trap micron-size IPGE (Os, Ir, Ru, Rh) alloys (e.g. Puchtel and Humayun, 2001; Righter et al., 2004; Brenan et al., 2003, 2005). In contrast, PGE $K^{\text{sulfide melt /silicate melt}}$ of the order of 1×10^4 - 10^6 indicate that PGE variations could easily be dominated by the presence of very small amounts of sulfides during differentiations (e.g. Peach et al., 1990, 1994; Bezman et al., 1994; Mungall and Brenan 2014). Overall, it appears that the silicate crystallization maximum at 63.5°N is not significantly affected by sulfides and PGE-alloys removal.

8. Sulfide removal effect.

Attempts to estimate the PGE enrichment of the Iceland mantle plume relative to the DMM source based on along-ridge basalt variation requires considering first the sulfide removal effect. The first question is whether these basalts are sulfide saturated or not. Sulfur variation along the ridge stays fairly constant (1000-1500 ppm range), until it drops drastically around 63°N (Fig 2, Forrest et al. 2017). The S-drop coincides with the onset of degassing of water, Cl (Fig 5d) and Br, as well as Se and Te, taking place at shallow water depths of eruption of 250-500 m (Unni and Schilling, 1978; Nichols et al., 2002; Forrest, 2005 and Forrest et al 2017). From 50°N to 63°N the S variation is clearly controlled by its solubility as sulfide-saturation, as also observed from other N-MORB (e.g. Mathez, 1976; Czamanske and Moore, 1977), and as vapor/melt

solubility further north and on Iceland. We now consider these two distinct end-member mixing regions separately.

8.1. Iceland.

Because of the degassing effect of S over and near Iceland, it is not possible to determine directly if the PGE Iceland basalts were sulfide-saturated at the time of eruption and need correction or not. Several workers have used Pd vs Cu diagrams to discriminate empirically between Sulfide-saturation from Sulfide-under-saturation, for subaerial S-outgassed basalts, by assuming that Cu is a non-volatile proxy for S (Fig.8) (Barnes, 1993; Vogel and Keays, 1997; Brooks et al., 1999; Woodland et al., 2002; Keays and Lightfoot, 2006). On this basis alone, as expected, it appears that the N- and T-MORB are all sulfide-saturated, whereas the Iceland basalts would be sulfide-unsaturated, with the exception of 2 or 3 more differentiated ones with lower than 7% MgO (Fig. 9). No sulfide-related PGE correction is considered necessary for our Iceland basalts, which stay essentially constant over the range of 7-10 % MgO (Fig. 9 a and b). This is fully consistent with Momme et al., (2003), who report Pd and Ir Iceland basalt variations staying essentially constant over a broader range of 7 -21 MgO % . A positive correlation of PGE with MgO would be expected if this were the case.

8.2. N-MORB from 50-54°N.

The extent of sulfide removal for this N-MORB population unaffected by the Iceland mantle plume is now considered. Fig 9 a and b shows that Ir and Pd of the Iceland group stay essentially constant with MgO, as expected for S-unsaturated basalts cooling and with silicate crystallization. Whereas in contrast within the N-MORB group, Ir and Pd in particular decrease with decreasing MgO, suggesting some sulfide removal as well. This is based on the fact that PGE partitions coefficients, $K^{\text{sulfide/silicate melt}}$ are so much greater than $K^{\text{silicate crystal/silicate melt}}$, as indicated earlier in section 5.3. This is further corroborated by the Cu vs MgO variation shown in Fig.8 c. As for Ir and Pd, Cu positively correlate with MgO for the S saturated N-MORB group, indicating some sulfide removal, since known sulfide liquid/silicate melt partition coefficients for Cu range from 827-1660 for basaltic melts with 9-12 FeO wt% (Mungall and Brenan 2014; Brenan 2015). In contrast, Cu in the S-unsaturated Iceland basalts negatively correlate with MgO, which is consistent with silicate fractionation without sulfide involvement.

Cu silicate crystal/ basaltic melt partition coefficient are all < 0.2 , including spinel (e.g. Liu et al. 2014 and Bougault and Hekinian, 1974). Finally, uranium, which is a highly incompatible in silicate and sulfide fractionations, negatively correlates with MgO in both the sulfide-unsaturated Iceland basalts and the sulfide-saturated N-MORB group, thus in full support of the above interpretation.

Bézos et al.(2005] estimated an immiscible sulfide melt segregation fraction, X_{sulfide} , of 120 ppm from the Pd content of a pair of N-MORB from the Kolbeinsey Ridge north of Iceland, ranging from 10 to 7 wt% MgO, and corresponding to a 54% crystallization of oliv-plag-cpx; resulting in a sulfide segregation rate of 2ppm/%FC (i.e. fractional crystallization). Their model assumed that: 1) no PGE partitioned into the silicate assemblage (i.e any silicate or oxide crystal/melt PGE partition coefficients are all zero; 2) a $K^{\text{sulfide/silicate melt}}$ of 35,000 for Pd.

For comparison using the same model, it can be shown that bracketing the positive PGE vs MgO trends shown in Fig.(8 a and b) for the N-MORB from 50-54°N would require a maximum sulfide melt segregation fraction of only 5-9 ppm and 17-36 ppm, based on their Ir and Pd contents, respectively (Table 1). These would correspond to a sulfide segregation of 0.1-0.3 ppm/%FC and 0.3-1.2ppm/%FC using Ir and Pd, respectively.

The two basalt pairs are: 1) the “initial” melt, TR 100 23D-10g, reached by ~37% oliv.-plag.-cpx crystallization, with the closely located “residual” basalt melt as EN025 1D-1g. 2) The initial melt TR138 7D-1Ag, located south of the Gibbs FZ, reached by ~53% silicate crystallization with the same residual melt as EN025 1D-1g (see Table 1 for PGE and MgO concentrations used in these calculations). The significant discrepancy from the sulfide removal rate estimate of Bézos et al., (2005) and ours is due to the fact that we used the PGE partition coefficients, $K^{\text{sulf. liq./sil.melt}}$, most recently reported by Mungall and Brenan (2014) which are 1-2 order of magnitude higher; namely averages of 4.58×10^5 and 1.89×10^5 for Ir and Pd for FeO in the range of 9-11 wt%.

In the remaining discussion, we will assume that only the local scatter about the large-scale along-ridge PGE and Cu trends observed (Figure 3) may be caused by fractional crystallization effects, sulfide-bearing or not, and that the large-scale trend is not predominantly driven by such effects.

9. Partial Melting

In order to account for the PGE gradients observed (Fig. 3a and b), we now consider “congruent” and “incongruent” melting models of a single “sulfide bearing” mantle source of Primordial Upper Mantle (PUM) composition with bulk silicate earth (BSE) PGE contents (i.e. BSE contains 250 ppm sulfur, or 714 ppm Fe- sulfide, McDonough and Sun, 1995), The models consider that the PGE are uniquely hosted in sulfides, and all silicates or oxides crystal/melt partition coefficients are zero, as has been previously assumed (e.g. Rehkämper et al., 1999; Bézou et al., 2005; Bockrath et al., 2004).

Increasing melting toward Iceland is evident from increasing crustal thickness, ridge elevation and related geophysical modeling (Vogt, 1971; Schilling, 1973; White et al. 1995, 1996; Ito et al., 1996, 1999; Smallwood et al., 1999; Searle et al., 1998). White et al., (1995) assumed a 200°C excess temperature for the Iceland plume and a melt thickness (basaltic crust) increasing from ~7km for normal oceanic crust thermally unaffected by the mantle plume to ~21km over the center of Iceland (see their Fig. 4). Empirically, we have scaled this crustal variation to a linear increase in the degree of melting F with latitude ($^{\circ}\text{N}$), namely $F = 0.066 + 0.00827(\text{Lat.}^{\circ}\text{N} - 50)$. For example, normal crust at 50°N is produced by a mean F of 6.6%, and over Iceland by 19%.

9.1. Congruent PGE sulfide liquid/silicate melt partitioning melting model.

This type of model has previously been discussed by Barnes et al., (1985); Mitchell and Keays, (1981); Fryer and Greenough, (1992]; Greenough and Owen (1992); Rehkämper et al., 1999b].

9.1.1. Pd and Ir variations

Figures 10a & b show the variations of BSE-normalized (Pd)_n and (Ir)_n observed in basalts from the Iceland SWNZ and the Reykjanes Ridge, as a function of the degree of melting F estimated from the thermal melting model of White et al., (1995). Superimposed on Figs. 10a & b are incremental sulfide-bearing partial melting models of the previously described PUM. Both a columnar and a pooled triangular decompression flow melting models are shown with distinct $K^{\text{sulfide liquid/silicate melt}}$ partition coefficients. A combination of the two dynamic flow models could satisfactorily bracket the range of PGE basalt variations observed and their inferred degrees of melting, providing the $K^{\text{sulfide liquid/silicate melt}}$ partition coefficients fall broadly in the range of 10^6 -

10^7 for Ir and 5×10^4 - 5×10^5 for Pd. The required $K^{\text{sulfide liquid/silicate melt}}$ partition coefficients are close to those recently reported by Mungall and Brenan (2014), which range from 6.7×10^4 - 5.4×10^5 (avg. 1.89×10^5) for Pd, and 4.8×10^4 - 1.9×10^6 (avg 4.58×10^5) for Ir. These are clearly more in line than those previously used in earlier melting models, such as 1×10^4 and 3.5×10^4 (e.g. Rehkämper et al. 1999b, Bézou et al 2005, Yang et al. 2014). However, in our model, the most depleted N-MORB from 50-54°N, unaffected by the Iceland mantle plume, would still require $K^{\text{sulfide liquid/silicate melt}}$ up to nearly a factor 10 higher for Ir and somewhat < 10 for Pd. This suggests that the DMM is depleted in PGE relative to the BSE values used for the PUM in this melting model.

9.1.2. Pd / Ir ratio variation for T-MORB and N-MORB

A similar problem is encountered when modeling the corresponding 10 to 300 (Pd/Ir)_n large range of variations observed in Fig. 10c for N-MORB and T-MORB. For comparison, Rehkämper et al., (1999) faced the same problem in modeling the smaller 23 to 62 (Pd/Ir)_n range they observed in basalts from Iceland and the Kolbeinsey Ridge, using $K^{\text{sulfide melt/silicate melt}}$ partitioning in the range of 10^4 to 10^5 . To alleviate the problem, they assumed that during partial melting Ir is also compatible in some non-sulfide mantle phases, namely olivine and spinel, while the bulk silicate crystal/melt D for Pd still remains equal to zero. A bulk silicate/melt partition coefficient D of 10, with a $K^{\text{sulfide melt/silicate melt}}$ of 1×10^4 for both Ir and Pd was required to reach the 23 to 62 (Pd/Ir)_n range they observed.. Along the same vein, Fig. 10c shows that our larger 10-300 (Pd/Ir)_n range observed for N-MORB and T-MORB can be modeled by fractional melting of a spinel lherzolite with PGE of BSE composition, within the range of the two columnar and triangular decompression flow melting regimes. It would require a bulk silicate crystal/melt D for Ir of 50, and $K^{\text{sulfide melt/silicate melt}}$ of 1×10^5 and 1×10^6 for Pd and Ir respectively. These $K^{\text{sulfide melt/silicate melt}}$ are again in more reasonable line with those of Mungall and Brenan (2104). If we consider Ir to be compatible in olivine only, as usually believed possible, an Ir bulk crystal/melt D of 94 would be required assuming a primitive spinel lherzolite mantle mineralogy and proportions similar to that used by Rehkämper et al. [1999b]). A $K^{\text{olivine/melt}}$ of 94 for Ir would be ~ 10 times higher than any reported and measured values (e.g. Naldrett and Barnes, 1986; Brenan et al., 2003, 2005), thus not likely. On the other hand, if Ir is compatible in spinel only, a $K^{\text{spinel/melt}}$ of 1667 would be required, which is within the range of measured and empirically modeled values by Righter et al., (2004), thus more likely.

Finally, we note that the N-MORB from 50-54°N in the range of 7-10% melting lie outside of the model's bounds and unexplained. Two solutions are in hand:

- 1) The simplest would be in the model parameters used. That is to compress the degree of melting range from 50-65°N to 10-19 % instead of the 6.6-19% based on White et al., (1995), which is acceptable considering the uncertainties involved.
- 2) Another possibility, unlikely and rejected, would be to consider a lower content for the PUM from 250 ppm used to 211 ppm recently suggested by Wang and Becker (2013). It would require that sulfide be exhausted at $F=17\%$ at 62.6°N and $F=8.5\%$ at only 52.3°N for the columnar and triangular mantle flow types, respectively. Beyond such sulfide exhaustions, the sulfur content would have to decrease in both cases, with increasing melting toward Iceland. This is clearly not the case as shown in Fig.2. North of 52.3°N S stays essentially constant. North of 62.6°N, S actually shows a slight increase up to the 63.5°N MgO minimum, and maximum extent of crystallization noted. (corresponding also to an FeO maximum, consistent with enhancing S-solubility (e.g. Haughton et al. 1974, Mathez, 1976). Northward of this critical region, as indicated early, S content drastically drops due to S degassing (i.e. vapor saturation).

9.1.3. Pd/ Ir ratio over Iceland.

The noticeable and unexpected low (Pd/Ir)_n of Iceland basalts relative to the T-MORB and even N-MORB shown in Fig. 10c needs consideration. It ranges between 30 to 120 for the Iceland SWNRZ, and about 10 -115 for overall Iceland tholeiitic basalts (Momme et al., 2003). The drop of (Pd/Ir)_n ratio over the Iceland SWRZ, results from the high spike of Ir relative to Pd, though both are enriched relative to N-MORB (Fig 3).

It is generally believed that the PGE fractionation patterns measured by the (Pd/Ir)_n is a function of the extent of melting F (e.g. Fryer and Greenough,1992; Greenough and Owen, 1992; Rehkämper et al., 1999b, Ely and Neal, 2003). Namely, the (PD/Ir)_n ratio is low in low- F alkali basalts, high in intermediate- F tholeiitic basalts, and upon sulfide exhaustion at $F > 25\%$, is again lower in komatiites.

We suggest that the drop in (Pd/Ir)_n over Iceland is a partial melting effect due to higher mean extent and pressure of melting over the rising mantle plume, dominated by the high-T-P melting within field of garnet stability, rather than the lower T-P melting spinel field along the Reykjanes Ridge. This is supported by: 1) The higher temperature and water content of the Iceland mantle

plume (Schilling et al. 1983; Poreda et al 1986; Schilling, 1991; Nichols et al. 2002). 2) The lower SiO₂ and Yb contents over Iceland, including the HREE cross-over patterns for basalts of the Iceland SWRZ relative to the Reykjanes Ridge N-MORB (Schilling et al., 1983). 3) Ir is compatible in spinel and to some extent retained in the mantle residue at lower degrees of melting (Richter et al., 2004), whereas to our knowledge there is no evidence that Ir and Pd is in garnet.

9.2.1. Incongruent melting of sulfide involving a residual Mss and sulfide melt.

PGE-constrained models of basalt generation by incongruent melting of a sulfide-bearing PUM, involving a monosulfide solid solution (Mss) coexisting with an immiscible sulfide melt, have been considered in broad terms by Mitchell and Keays (1981), Fryer and Greenough (1992), Greenough and Owen (1992), Ballhaus (1995), and Alard et al. (2000). We now consider the quantitative incongruent sulfide-bearing PUM melting model of Bockrath et al. (2004) and Ballhaus et al. (2006) for the case of Ir and Pd. Their model involves formation of a residual Mss phase coexisting with an immiscible sulfide melt, which is physically entrained and diluted with increasing degree of silicate melting. According to this physical, non-equilibrium model, they point out that PGE would decrease and behave as incompatible elements with increasing silicate melting. Testing of this model requires knowing $K^{Mss/sulfide\ melt}$ for Ir and Pd. Barnes and Maier, (2000) and Ballhaus, (2006) report a range of measured $K^{Mss/sulfide\ melt}$ of 0.9-10 for Ir and 0.03-0.2 for Pd, for S-saturated runs.

Using the $K^{Mss/sulfide\ melt}$ for Ir and Pd of 10 and 0.14, respectively, and a sulfide melt fraction F_{sulf} varying from 0.01 to 1 (Bockrath et al. (2004, used 0.5)) show parallel trends opposite or orthogonal to that of the Pd and Ir basalt data from the Reykjanes Ridge and the Iceland SWNZ, respectively (Fig 11). Their model must be rejected for the Iceland-Reykjanes Ridge, as also evident from the highly incompatible elements increasing toward Iceland observed on the same samples, such as Th, U, Nd, etc. (Kelley et al. 2013)

9.2.2. Incongruent melting of sulfide involving a residual alloy and sulfide melt.

We have also tested the Ballhaus, [1995] model of incongruent melting of sulfide into an alloy and a coexisting sulfide melt for Reykjanes Ridge N-MORB. We assumed Barnes and Maier (2000) reported partition coefficient $K^{alloy/sulfide\ melt}$ in the range of: 1) 50-324 for Ir, and 2)

0.04-2.6 for Pd. Under these conditions we obtain too high values in the silicate melt for the Reykjanes Ridge N-MORB, namely: 1) (Pd)_n values of 4.81-1.39, compared to the observed range of 7.7×10^{-3} to 4.6×10^{-1} ; 2) (Ir)_n values of $0.975-1 \times 10^{-2}$, compared to the observed range of 3×10^{-4} to 4×10^{-3} .

Clearly, in either case the model could not generate the very low (Ir)_n and (Pd)_n values observed in the Reykjanes Ridge N-MORB.

Based on the above modeling, the model of incongruent melting of sulfide involving a residual alloy and sulfide melt is also found inadequate in accounting for the very low PGE contents of the Reykjanes Ridge N-MORB.

Finally, we found that the incongruent sulfide melting model of Rehkämper et al. (1999), involving PGE alloys as the residual phase, would produce PGE concentrations two orders of magnitude higher than observed for the Reykjanes Ridge N-MORB.

We conclude that the three types of partial melting models considered in this section, namely increasing degree of partial melting toward the Iceland hotspot of a single sulfide-bearing mantle source of PUM composition cannot reasonably account for the PGE gradient observed toward Iceland. Clearly, a DMM mantle source with lower PGE content is required to account for the very low PGE content of the 50-54°N Reykjanes Ridge N-MORB unaffected by the Iceland mantle plume.

10. PGE Two-source Mixing Model Evaluation.

The chemical and isotopic make up of the Iceland mantle plume is complex and controversial. From a Pb isotope perspective basalts on Iceland from tertiary to present suggest at least three distinct end-member components (Hanan and Schilling, 1997). More components have been proposed which would reflect the chemical and isotopic complexity of old recycled oceanic lithosphere, and mantle entrainment into the plume as it rises from the core/mantle boundary (CMB) (e.g. Hoffmann and White, 1982; Chauvel and Hémond, 1999; Skovgaard et al., 2001). It may also involve mixing with a sub-continental component embedded in the DMM lithosphere due to the proximity to and young age of opening of the Atlantic in the region (Schilling et al., 1999; Hanan et al., 2000; Debaille et al., 2009). Yet, mixing along the Reykjanes Ridge southward appear essentially and dominantly binary on the basis of long-wave-

length isotopic variations (Hart et al., 1973; Sun et al., 1975; Poreda et al., 1986; Hilton et al., 2000; Blichert-Toft et al., 2005), except occasionally locally (Murton et al., 2002; Thirlwall et al., 2004).

Geochemical tests of binary mixing in scatter diagrams of elements A/B versus 1/B and A/B versus C/B variations must be linear (Langmuir et al., 1978), providing that mixing is the last magmatic operative process. This can hardly be the case along the 1900 km length-scale considered here, as evident for example by the local and pronounced late-stage, low pressure magma crystallization evolution observed on either side of 63.5°N (Figs. 3 a & b), and of course varying partial melting. This is evident by the lack of co-variation in A/B versus 1/B diagram involving PGE, Ni and Cu, which revealed r^2 linear correlation coefficient all less than 0.079. The exceptions are: 1) Cu/Pd versus 1/Pd, with an r^2 of 0.93 for two elements which are both similarly incompatible in silicate relative to sulfides, and 2) Ni/Ir versus 1/ Ir, with a r^2 of 0.92, for two elements which are relatively mildly compatible in silicates relative to sulfides.

Linear A/B versus C/B co-variations among inter PGE's ratios are more acceptable. They linearly co-vary with r^2 in the range of 0.31 to 0.78, apparently because of their similar behavior in systems controlled by sulfide/melt partitioning. The great sensitivity of PGE-bearing sulfide and PGE-alloys fractionation during partial melting and crystallization clearly prevent conclusive tests for binary mixing, but does not rule out mixing in the mantle at some stage.

In fact, the Ir, Pd, Cu and U variations with MgO shown in Fig 9, clearly indicate that independently of MgO variation, the Iceland basalts are systematically richer than the 50-64°N N-MORB group unaffected by the Iceland mantle plume. This clearly suggests that these elements are derived from two distinct mantle sources, namely, the Iceland mantle plume and the DMM source, whether compatible or incompatible elements are considered.

11. Discussion and conclusions.

As indicated earlier, our interpretation of the data reported emphasizes primarily the relative PGE, Re, Cu, Ag and Cd spatial variations observed. This is only possible, considering the nature of our overall sampling-scale (~1665 km long) and interval sampling-scale (~31 km on average). None of the samples considered are likely to be consanguineous and adequate for evaluating directly, or correcting for, local effects, such as fractional crystallization and sulfide melt removal.

Two distinct models, not necessarily mutually exclusive were considered:

1) Two distinct Pd and Ir mantle sources and their mixing along the ridge, as previously evident from Pb-Nd-Sr-He isotope and (La/Sm)_n variations of the same samples. In brief, this is supported by the systematic Ir and Pd variations with MgO (Fig 8). The PGE in the Iceland basalts stay essentially constant with MgO, as expected for S-unsaturated basalts. Whereas in contrast the 50-54°N N-MORB group unaffected by the Iceland mantle plume are systematically lower by a factor of ~10-15 in Pd and Ir, and decrease with decreasing MgO, suggesting sulfide saturation and removal. T-MORB lie broadly in between the Iceland and the 50-54°N N-MORB groups, as expected for binary mixing.

2) Possibly, increasing partial melting towards Iceland of a uniform sulfide-bearing primary mantle source (PUM) with PGE content hosted entirely in the sulfide. We show that the extremely low PGE contents of the 50-54°N N-MORB, unaffected by the Iceland mantle plume, cannot be accounted for by such partial melting model, even with the highest $K^{\text{sulfide melt/silicate melt}}$ of 1×10^5 and 1×10^6 for Pd and Ir recently reported by Mungall and Brenan, (2014), compared to $\sim 1-5 \times 10^4$ previously considered (e.g. Peach et al., 1994; Rehkämper et al., 1999; Bézou et al., 2005). This is not to suggest that increasing melting toward Iceland is not a factor as well. It most likely is.

Finally, we note that the extent of the PGE, Cu, Ag, Re and Cd depletions in the DMM relative to the Iceland mantle plume source remains model dependent, including the northward increasing melting percent assumed, and cannot be quantified at this point. Detailed modeling is required involving melting in the garnet field under Iceland and the spinel field under the Reykjanes Ridge, as apparent from the Re, Pd/Ir, SiO₂ and Yb with HREE cross-over patterns variations observed.

Ag follows closely Cu variation along the Reykjanes Ridge, whereas Cd shows an intermediate behavior between Cu and Re, and may also have been affected by subaerial degassing, as Re and other volatiles, such as water, Cl, Br and S.

Finally we also show that fractional crystallization of silicates involving PGE-rich immiscible sulfides has limited effects on the PGE, Cu, Ag, Re and Cd large-scale gradients observed along the Reykjanes Ridge, with the possible exception of Ru, which shows very large overall scatter.

Acknowledgments.

We thank the National Science Foundation for their strong support through grants OCE9906799 and OCE0326658 to the authors. We also thank the investigators that worked to verify our analytical protocols through the interlaboratory analysis of our in-house MORB standard for PGEs. They were: T. Meisel at Univ. Loeben; B. Peucker-Ehrenbrink at WHOI; A. Bezos at LGM-IPGP; S. Escrig at LM-CNRS and LGC-IPGP; A. Gannoun at Open Univ.; and M. Humayun and I. Puchtel at Univ. of Chicago. B. Peucker-Ehrenbrink is further thanked for providing a combined PGE spike solution for in-depth calibration of our own solution. Finally, Dr. J. Morgan of Colorado State Univ. is also acknowledged for generously providing us with a clean ^{191}Ir spike solution that was used for the Ir isotope dilution analyses. JGS thanks Magdalena Andres for help with the modeling.

List of Tables

Table 1. PGE, Re, Ni, Cu, Ag and Cd basalt contents from the Reykjanes Ridge and Iceland S.W. Neovolcanic Rift Zone, from 50°N to 65°N

Figure Captions

Fig. 1. Seafloor relief map based on free-air gravity anomalies (Smith and Sandwell, 1994). Basalt sample locations for this study are shown along the Reykjanes Ridge and extension over Iceland SW Neovolcanic Zone (SWNZ). Color coding is based on the mixing model of the Iceland mantle plume (red), depleted upper mantle (blue), and mixing zone (green), based on (La/Sm)_n variations (Schilling, 1973). The same symbols are used in all the subsequent figures.

Fig. 2. Reykjanes Ridge-Iceland latitudinal basalt glass variations in $^{206}\text{Pb}/^{204}\text{Pb}$, (Blichert-Toft et al., 2005), $^3\text{He}/^4\text{He}$ (R/Ra) (Kurz et al., 1985; Poreda et al., 1986), sulfur content, S, [Forrest, 2005; Forrest et al., 2017], and dredged sample elevations (Schilling et al., 1983). Note that the MORB glasses are sulfide-saturated. Over Iceland, are vapor/melt saturated due to degassing, as for water. Basalts with <250ppm S are subaerially erupted, whereas those with >480ppm S are glasses subglacially erupted and less degassed due to higher overburden pressures (Moore and Calk, 1991 - see Section 8).

Fig. 3.1. Reykjanes Ridge-Iceland latitudinal basalt glass variations in: Pt, Pd and corresponding Mg-value. Note the Mg-value minimum at 63.5 °N.

Fig. 3.2. Reykjanes Ridge-Iceland latitudinal basalt glass variations in: Os, Ir and Ru.

Fig. 3.3. Reykjanes Ridge-Iceland latitudinal basalt glass variations in: Cu, Ag and Ni. Note the Ni minimum at 63.5 °N, as also evident in the Mg-value (Fig. 3.1); (or MgO and Cr, not shown)

Fig. 4. Reykjanes Ridge-Iceland latitudinal basalt glass variations in: Re, SiO₂, Yb, and Cd. Note the Re increase northward as for other PGE (Fig.3) but its drastic drop over Iceland, as well as SiO₂, Yb, and to some extent Cd, though the last three elements stay essentially constant along the Reykjanes Ridge. See text for probable causes of these variations, including retention by garnet.

Fig. 5. Reykjanes Ridge-Iceland latitudinal basalt glass variations for: a,b&c) Re/Yb, Re/Ir and Cu/Re ratios, respectively. The Re/Yb ratio variation is dominated by that of Re shown in Fig.4. In, contrast Re/Ir and Cu/Re stay essentially constant along the Reykjanes Ridge, while the four elements increase northward along the ridge (Fig 3 and 4), until Re drastically drop over Iceland (Fig.4); d) Cl whole-rock basalt contents (Unni, 1976). The drastic Cl decrease near and over Iceland is also apparent in S (Fig.2) and H₂O (not shown). These have been attributed to volatile degassing (Unni and Schilling 1978, Forrest et al., 2017) and could also be attributed to Re volatility. See text for further details.

Fig. 6b&c. Re and Cu/Re covariations with Cl content in SW Iceland rift zone (filled red circles), and Reykjanes Ridge samples erupted at water depths less than 500m (>63°N) (green filled triangles). Cl data from (Unni, 1976; Unni and Schilling, 1978). Note the excellent positive correlation of Re with Cl and the inverse one of Cu/Re with Cl. For reference, Fig 6a shows the location and elevation of these degassed basalts and those erupted deeper along the Reykjanes Ridge (black dots). For a full elevation profile with latitude see Fig. 2.

Fig. 7. BSE-normalized Ni-PGE-Cu enrichment patterns from the Reykjanes Ridge- Iceland sampling shown in Fig.1, using the same sample color coding for the 3 groups.

Fig. 8. Cu vs. Pd for the Reykjanes Ridge-Iceland basalts. Cu is taken as a non-volatile proxy for sulfur in discriminating sulfide-saturated from sulfide-undersaturated magmas (Vogel and Keays, 1997). This empirical dividing line is taken from Keays and Lightfoot [2006]. It is based on subaerially erupted flood basalts from West and East Greenland and the Siberian traps. On this basis alone, most of the Iceland SWNZ basalts were sulfide-undersaturated prior outgassing of volatiles, including S. (for comparison see S variation in Fig.2). The N-MORB Reykjanes Ridge field is sulfide-saturated and comparable to other MORB from the Atlantic, Pacific and Indian Ocean Ridges reported by Rehkämper et al.,(1999b) and Bézou et al., (2005), (i.e. Cu range: ~50–110ppm, Pd range: ~0.001-2 ppb). See text for further details.

Fig. 9. Ir, Pd, Cu, U, variations with MgO, for the sulfide-unsaturated Iceland basalts (red symbols) and the sulfide-saturated N-MORB group from 50-54°N, unaffected by the Iceland mantle plume (blue symbols). Note that the Ir, Pd and Cu positively correlate with MgO for the S-saturated N-MORB group (i.e., some sulfide removal), whereas in the sulfide-unsaturated Iceland basalts Ir and Pd remain essentially constant and Cu correlates slightly negatively with MgO. On the other hand, U, which is a highly incompatible in silicate and sulfide fractionations,

correlates negatively with MgO in both the sulfide-unsaturated Iceland basalts and the sulfide-saturated N-MORB group. See text for further details.

Fig. 10a. Reykjanes Ridge-Iceland basalts BSE normalized $(Pd)_n$ vs degree of melting F . F is assumed to increase linearly with latitude $^{\circ}N$ (i.e. $F = 0.066 + 0.00827 (\text{Lat.}^{\circ}N - 50)$, modified after the thermal melting model of White et al., (1995). See text for justification. Superimposed are columnar and triangular flow, sulfide mantle bearing melting models, modified after Rehkämper et al. (1999b). We simply used a non-modal incremental batch melting model with a continuous 0.001 melt fraction retention. Results are hardly distinguishable. Conditions used, up to $F= 20\%$ when the mantle sulfide is exhausted, are:

Phases:	silicate solid	Retained melt	sulfide
K_j	0	1	10^4 to 10^6
solid(xoj)	0.994286	0.001	0.000714
melt(pj)	0.99643		0.00357

Note that $K(\text{sulfide /melt})$ of the order of 10^6 would be required to span the N-MORB Reykjanes Ridge Pd data variation observed! See text for further implications.

Fig.10b. Reykjanes Ridge-Iceland basalts BSE normalized $(Ir)_n$ vs. degree of melting F . The same model parameters described in Fig10a are used. However, the $K(\text{sulfide/melt})$ range for Ir must be extended to 10^7 to span the N-MORB Reykjanes Ridge Ir data variation observed! See text for further implications.

Fig.10c. Reykjanes Ridge-Iceland basalts BSE normalized $(Pd/Ir)_n$ ratio vs degree of melting F , as in Fig.10a&b. Superimposed are the same columnar and triangular flow sulfide melting model shown in Fig 10a&b, but assuming this time a bulk $K(\text{silicate crystal/melt})$ for Ir of 50 rather than zero, still zero for Pd, and $K(\text{sulfide/melt})$ of 10^5 and 10^6 for Pd and Ir, respectively. See text for implications.

Fig.11. a&b. Reykjanes Ridge and Iceland basalt variations Ir_n and Pd_n , normalized to BSE as a function of melt fraction F increasing toward Iceland (as assumed and used in Figure 10). Symbol colors are the same as in Figure 1. Superimposed is the non-equilibrium physical incongruent sulfide-bearing PUM melting model of Bockrath et al. [2004] and Ballhaus et al. [2006]. The different curves refer to the weight fractions of sulfide (f_{sul}) initially being melted according to their model. They assumed 0.5. Note that the trends predicted by this model are opposite or orthogonal to that observed along the Reykjanes Ridge and Iceland, respectively; assuming that melting increases toward the Iceland plume.

References

- Alard, O., Griffin, W.L., Lorand, J.P. Jackson, S.E. and O'Reilly, S.Y., 2000. Non-chondritic distribution of the highly siderophile elements in mantle sulphides, *Nature*, 407, 891-894.
 Ballhaus, C., Is the upper mantle metal-saturated? (1995) *Earth Planet. Sci. Lett.*, 132, 75-86.

- Ballhaus, C., Bockrath, C. Wohlgemuth-Ueberwasser, C., Laurenz, V., J. Berndt, J. (2006) Fractionation of the noble metals by physical processes, *Contrib. Mineral. Petrol.*, 152, 667-684.
- Barnes, S.-J., Naldrett, A.J., Gordon, M.P., 1985. The origin of the fractionation of platinum-group elements in terrestrial magmas, *Chemical Geology*, 53, 303-323.
- Barnes, S.-J., 1993. Partitioning of the platinum group elements and gold between silicate and sulphide magmas in the Munni Munni Complex, Western Australia, *Geochim. Cosmochim. Acta*, 57, 1277-1290.
- Barnes, S.-J., Maier, W.D., 2000. The fractionation of Ni, Cu and the noble metals in silicate and sulfide liquids. In *Dynamic Processes in Magmatic Ore Deposits and their application in mineral exploration.*, Ed. Keays, R.R., Leshner, C.M., Lightfoot, P.C. et Farrow, C.E.G., Geological Association of Canada, Short Course 13, 69-106.
- Bennett, V.C., Norman, M.D., Garcia, M.O., 2000. Rhenium and platinum group element abundances correlated with mantle source components in Hawaiian picrites: sulphides in the plume, *Earth Planet. Sci. Lett.*, 183, 513-526.
- Bezmen, N.I., Asif, A., Brüggmann, G.E., Romanenko, I.M., Naldrett, A.J., 1994. Distribution of Pd, Rh, Ru, Ir Os and Au between sulfide and silicate metals, *Geochim. Cosmochim. Acta*, 58, 1251-1260.
- Bézos, A., Lorand, J.-P., Humler, E. Gros, M., 2005. Platinum element group systematics in Mid-Ocean Ridge basaltic glasses from the Pacific, Atlantic, and Indian Oceans, *Geochim. Cosmochim. Acta*, 69, 2613-2627.
- Blichert-Toft, J., Agranier, A., Andres, M., Kingsley, R., Schilling, J.-G., Albarede, F., 2005. Geochemical segmentation of the Mid-Atlantic Ridge north of Iceland and ridge-hot spot interaction in the North Atlantic, *Geochem. Geophys. Geosyst.* 6, 1-27.
- Bockrath, C., Ballhaus, C., Holzheid, A., 2004. Fractionation of the Platinum-Group Elements During Mantle Melting, *Science*, 305, 1951-1953.
- Bougault H., Hekinian R., 1974. Rift valley in the Atlantic Ocean near 36°50'N: Petrology and geochemistry of basaltic rocks. *Earth Planet. Sci. Lett.* 24, 249-261.
- Brandon, A.D., R.J. Walker, J.W. Morgan, M.D Norman, and H.M. Prichard, 1998, Coupled ¹⁸⁶Os and ¹⁸⁷Os evidence for core-mantle interaction, *Science*, 280, 1570-1573
- Brenan, J.M., 2015. Se-Te fractionation by sulfide-silicate melt partitioning: Implications for the composition of mantle-derived magmas and their melting residues, *Chemical Geology.*, in press
- Brenan, J.M., McDonough, W. F., Dalpe, C., 2003. Experimental constraints on the partitioning of rhenium and some platinum-group elements between olivine and silicate melt, *Earth Planet. Sci. Lett.*, 212, 135-150.
- Brenan, J.M., McDonough, W. F. Ash, R., 2005. An experimental study of the solubility and partitioning of iridium, osmium and gold between olivine and silicate melt, *Earth Planet. Sci. Lett.*, 237, 855-872.
- Brooks, C. K., Keays, R.R., Lambert, D. D., Frick, L.R., Nielsen, T.F.D., 1999. Re-Os isotope geochemistry of Tertiary picritic and basaltic magmatism of East Greenland: constraints on plume-lithosphere interactions and the genesis of the Platinova reef, Skaergaard intrusion, *Lithos* 47, 107-126.
- Chauvel, C., Hémond, C., 2000. Melting of a complete section of recycled oceanic crust: Trace elements and Pb isotopic evidence from Iceland, *Geochem. Geophys. Geosyst.*, 1, , doi: 1999GC000002.

- Chou, C.-L., Shaw, D.M., Crocket, J.H., 1983. Siderophile trace elements in the earth's oceanic crust and upper mantle, Proc. Lunar Planet. Sci. Conf., 88, A507-A518.
- Crocket, J.H., 1981. Geochemistry of the platinum-group elements, Can. Inst. Min. Metall., Spec. Iss. 23, 47-64.
- Crocket, J.H., 2000. PGE in fresh basalt, hydrothermal alteration products, and volcanic incrustations of Kilauea volcano, Hawaii, 64, 1791-1807.
- Czamanske, G.K., Moore, J.G., 1997. Composition and phase chemistry of sulfide globules in basalt from the Mid-Atlantic Ridge rift valley near 37°N latitude, Geol. Soc. Am. Bull., 88, 587-599.
- Debaille, V., Tronnes, R.G., Brandon, A. D., Waight, T. E., Graham, D. W., Lee, C. T-A., 2009. Primitive off-rift basalts from Iceland and Jan Mayen: Os-isotopic evidence for a mantle source containing enriched subcontinental lithosphere, Geochim. Cosmochim. Acta, 73, 3423-3449.
- Ely, J.C., Neal, C.R., 2003. Using platinum-group elements to investigate the origin of the Ontong Java Plateau, SW Pacific, Chemical Geology, 196, 235-257.
- Fisk, M. R., 1978. Melting relations and mineral chemistry of Iceland and Reykjanes Ridge basalts, PhD. Dissertation, University of Rhode Island, 254 pages.
- Fisk, M.R., Schilling, J.-G., Sigurdsson, H., 1980. An experimental investigation of Iceland and Reykjanes Ridge Tholeiites: I. Phase relations, Contrib. Mineral. Petrol., 74, 361-374.
- Forrest, A. M., 2005. Sulfur, Selenium and Tellurium in Reykjanes Ridge and Iceland Basalts, M.S. Thesis, Graduate School of Oceanography, University of Rhode Island, Kingston RI, 02881. 175 pages.
- Forrest, A. M., Kelley, K.A., Schilling, J.-G., 2017. Selenium, tellurium and sulfur variations in basalts along the Reykjanes Ridge and extension over Iceland, from 50°N to 65° N. Chemical Geology, under review.
- Fryer, B.J., Greenough, J.D., 1992. Evidence for mantle heterogeneity from platinum-group-element abundances in Indian Ocean basalts, Can. J. Earth Sci., 29, 2329-2340.
- Govindaraju, K., 1994. Compilation of working values and sample description for 383 geostandards, Geostand. Newsl., 18, 1-158.
- Greenough, J.D., Owen, J.V., 1992. Platinum-group element geochemistry of continental tholeiites: Analysis of the Long Range dyke swarm, Newfoundland, Canada, Chemical Geology, 98, 203-219.
- Guo, J.F., Griffin, W.L., O'Reilly, S.Y., 1999. Geochemistry and origin of sulphide minerals in mantle xenoliths: Qilin, southeastern China. Journal of Petrology, 40, 1125-1149.
- Hanan, B.B. Schilling, J.-G. (1997) The dynamic evolution of the Iceland mantle plume: the lead isotope perspective, Earth Planet. Sci. Lett., 151, 43-60.
- Hanan, B. B., Blichert-Toft, J. Kingsley, R. Schilling, J.-G., 2000. Depleted Iceland mantle plume geochemical signature: Artifact of multicomponent mixing?, Geochim. Geophys. Geosyst., 1 DOI: 10.1029/1999GC000009
- Hart, S.R., Ravizza, G.E., 1996. Os partitioning between Phases in Lherzholite and Basalts, in Earth Processes: Reading the isotopic code, Geophysical Monograph 95, AGU, pp. 123-134.
- Hart, S.R., Schilling, J.-G., Powell, J.L., 1973. Basalts from Iceland and along the Reykjanes Ridge: Sr isotope geochemistry, Nature Phys. Sci., 236, 104-107.
- Hassler, D.R., Peucker-Ehrenbrink, B., Ravizza, G., 2000. Rapid determination of Os isotopic composition by sparging OsO₄ into a magnetic-sector ICP-MS, Chem. Geol., 166, 1-14.

- Haughton, D.R., Roeder, P.L., Skinner, B.J., 1974. Solubility of Sulfur in Mafic Magmas. *Economic Geology*, 69(4): 451-467.
- Hauri, E., Hart, S.R., 1997. Rhenium abundances and systematics in oceanic basalts, *Chem. Geol.* 139, 185-205, 1997.
- Hermes, O.D., Schilling, J-G., 1976. Olivine from Reykjanes Ridge and Iceland Tholeiites, and its significance to the Two-Mantle Source Model, *Earth Planet. Sci. Lett.*, 28, 345-355.
- Hertogen, J., Janssens, M.-J., Palme, H., 1980. Trace elements in ocean ridge basalt glasses: implications for fractionations during mantle evolution and petrogenesis, *Geochim. Cosmochim. Acta*, 44, 2125-2143.
- Hilton, D. R., Thirlwall, M.F., Taylor, R.N., Murton, B.J., Nichols, A., 2000. Controls on magmatic degassing along the Reykjanes Ridge with implications for the helium paradox, *Earth Planet. Sci. Lett.*, 183, 43-50.
- Hofmann, A.W., White, W.M., 1982. Mantle plumes from ancient oceanic crust. *Earth and Planetary Science Letters*, 57: 421-436.
- Ito, G., Lin, J., Gable, C. W., 1996. Dynamics of mantle flow and melting at a ridge-centered hotspot: Iceland and the Mid-Atlantic Ridge, *Earth Planet. Sci. Lett.*, 144, 53-74.
- Ito, G., Shen, Y., Hirth, G, Wolfe, C. J., 1999. Mantle flow, melting, and dehydration of the Iceland mantle plume, *Earth Planet. Sci. Lett.*, 165, 81-96.
- Jagoutz, E., Palme, H., Baddenhausen, H., Blum, K., Cendales, M., Dreibus, G., Spettel, B., Lorenz, V., Wänke, H., 1979. The abundances of major, minor and trace elements in the earth's mantle as derived from primitive ultramafic nodules, *Proc. Lunar Planet. Sci. Conf.*, 10th, 2031-2050.
- Keays, R.R., 1995. The role of komatiitic and picritic magmatism and S-saturation in the formation of ore deposits, *Lithos*, 34, 1-18.
- Keays, R. R., Lightfoot, P.C., 2006. Siderophile and chalcophile metal variations in Tertiary picrites and basalts from West Greenland with implication for the sulfide saturation history of continental flood basalt magmas, *Miner. Deposita*, 4, 319-336.
- Kelley, K.A., Kingsley, R.H., Schilling, J.-G., 2013. Composition of plume-influenced mid-ocean ridge lavas and glasses from the Mid-Atlantic Ridge, East Pacific Rise, Galápagos Spreading Center, and Gulf of Aden. *Geochemistry Geophysics Geosystems*, 14(1), DOI:10.1002/ggge.20049.
- Kingsley, R., Bézou, A., Escrig, S., Gannoun, S., Humayun, M., Meisel, T., Peucker-Ehrenbrink, B., Puchtel, I., Sharma, M., Schilling, J.-G., 2004, Interlaboratory Comparison of PGE and Re in a Mid-Ocean Ridge Basalt, EOS, Transactions, American Geophysical Union, 85, Spring Meeting.
- Kurz, M. D., Meyer, P.S., Sigurdsson, H., 1985. Helium isotopic systematics within the neovolcanic zones of Iceland, *Earth Planet. Sci. Lett.*, 74, 291-305.
- Langmuir, C. H., Vocke, R. D., Hanson, G. N., Hart, S. R., 1978. A general mixing equation with applications to Icelandic basalts, *Earth Planet. Sci. Lett.*, 37, 380-392.
- Lassiter, J.C., 2003. Rhenium volatility in subaerial lavas; constraints from subaerial and submarine portions of the HSDP-2 Mauna Kea drill core, *Earth and Planetary Science Letters*, 214.311-325.
- Liu, X, Xiog, X., Audétat, A., Li, Y., Song, M., Li, L., Sun, W., X., 2014. Ding, Partition of copper between olivine orthopyroxene, clinopyroxene, spinel and garnet and silicate melts at upper mantle conditions, *Geochim. Cosmochim. Acta*, 125,1-22.

- Lorand, J.P., Alard, O., 2001. Geochemistry of platinum-group elements in subcontinental lithospheric mantle: in-situ and whole-rock analyses of some spinel peridotite xenoliths, Massif Central, France. *Geochim. Cosmochim. Acta* 65, 2789-2806.
- Lorand, J.P., Gros, M., Pattou, L., 1999. Fractionation of platinum-group elements in the upper mantle: a detailed study in Pyrenean orogenic peridotites, *J. Petrol.*, 40, 951-987.
- Lorand, J.P., Luguët, A., Alard, O., Bézou, A., Meisel, T., 2008. Abundance and distribution of platinum-group elements in orogenic lherzolites: a case study in a Fontete Rouge lherzolite (French Pyrénées) *Chemical Geology*, 248, 174-194.
- Luguët, A., Lorand, J. P., Seyler, M., 2003. Sulfide petrology and highly siderophile element geochemistry of abyssal peridotites: A coupled study of samples from the Kane Fracture Zone (45°W 23°20N, MARK Area, Atlantic Ocean), *Geochim. Cosmochim. Acta*, 67, 1553-1570.
- Luguët, A., Alard, O., Lorand, J.P., Pearson, N.J., Ryan, C., O'Reilly, S.Y., 2001. Laser-ablation microprobe (LAM)-ICPMS unravels the highly siderophile element geochemistry of the oceanic mantle, *Earth and Planetary Science letters*, 189, 285-294.
- Mathez, E.A., 1976. Sulfur solubility and magmatic sulfides in submarine basalt glass, *J. Geophys. Res.*, 81, 4269-4276.
- McDonough, W.F., Sun, S.-S., 1995. The composition of the earth, *Chem. Geol.*, 120, 223-253.
- Mitchell, R.H., Keays, R.R., 1981. Abundance and distribution of gold, palladium and iridium in some spinel and garnet Lherzolites: implications for the nature and origin of precious metal-rich intergranular components in the upper mantle, *Geochim. Cosmochim. Acta*, 45, 2425-2442.
- Momme, P., Oskarsson, N., Keays, R.R., 2003. Platinum-group elements in the Iceland rift system: melting processes and mantle source beneath Iceland, *Chemical Geology*, 196, 209-234.
- Moore, J.G., Calk, L.C., 1991. Degassing and differentiation in subglacial volcanoes, Iceland, *J. Volcanol. Geotherm. Res.*, 46, 157-180.
- Moore, J.G., Schilling, J.-G., 1973. Vesicles, water and sulphur in Reykjanes Ridge basalts, *Contrib. Mineral. Petrol.*, 41, 105-118.
- Morgan, J.W., 1986. Ultramafic Xenoliths: Clues to Earth's late accretionary history, *J. Geophys. Res.*, 91, 12375-12387.
- Morgan, J.W., Wandless, G.A., Petrie, R.K., Irving, A.J., 1981. Composition of the Earth's upper mantle - I. Siderophile trace elements in ultramafic nodules, *Tectonophysics*, 75, 47-67.
- Mungall, J.E., Brenan, J.M., 2014. Partitioning of platinum-group elements and Au between sulfide liquid and basalt and origins of mantle-crust fractionation of chalcophile elements, *Geochim. Cosmochim. Acta*, 125, 265-289.
- Murton, B.J., Taylor, R.N., Thirlwall, M.F., 2002. Plume-Ridge Interaction: a Geochemical Perspective from the Reykjanes Ridge, *Journal of Petrology*, 43, 1987-2012.
- Naldrett, A.J., S.-J. Barnes, 1986. The behavior of platinum group elements during fractional crystallization and partial melting with special reference to the composition of magmatic sulfide ores, *Fortschr. Miner.* 64, 113-133.
- Nichols, A.R.L., Carroll, M. R., Hoskuldsson, A., 2002. Is the Iceland hot spot also wet? Evidence from the water contents of undegassed submarine and subglacial pillow basalts, *Earth and Planet. Sci. Lett.*, 202, 77-87.

- Pattou, L., Lorand, J.P., Gros, M., 1996. Non-chondritic platinum-group element ratios in the Earth's mantle, *Nature*, 379, 712-715.
- Peach, C.L., Mathez, E.A., Keays, R.R., 1990. Sulfide melt-silicate melt distribution coefficients for noble metals and other chalcophile elements as deduced from MORB: Implications for partial melting, *Geochim. Cosmochim. Acta*, 54, 3379-3389.
- Pearson, D.G., Woodland, S.J., 2000. Solvent extraction/anion exchange separation and determination of PGE's (Os, Ir, Pt, Pd, Ru) and Re-Os isotopes in geological samples by isotope dilution ICP-MS, *Chem. Geol.*, 165, 87-107.
- Pearson, D.G., Irvine, G.J., Ionov, D.A., Boyd, F.R., Dreibus, G.E., 2004. Re-Os isotope systematics and platinum group element fractionation during mantle melt extraction: a study of massif and xenolith peridotite suites, *Chemical Geology*, 208, 29-59.
- Poreda, R., Schilling, J.-G. Craig, H., 1986. Helium and hydrogen isotopes in ocean-ridge basalts north and south of Iceland, *Earth Planet. Sci. Lett.*, 78, 1-17.
- Puchtel, I.S., and M. Humayun, Platinum group element fractionation in a komatiitic basalt lava lake, *Geochim. Cosmochim. Acta*, 65, 2979-2993, 2001.
- Rehkämper, M., Halliday, A.N., Barfod, D., Fitton, J.G., Dawson, J.B., 1997. Platinum-group element abundance patterns in different mantle environments, *Science*, 278, 1595-1598.
- Rehkämper, M., Halliday, A.N., Alt, J., Fitton, J.G., Zipfel, J., Takazawa, E., 1999a. Non-chondritic platinum-group element ratios in oceanic mantle lithosphere; petrogenetic signature of melt percolation? *Earth Planet. Sci. Lett.*, 172, 65-81.
- Rehkämper, M., Halliday, A.N., Fitton, J.G., Lee, D.C., Wieneke, M., Arndt, N.T., 1999b. Ir, Ru, Pt, and Pd in basalts and komatiites; New constraints for the geochemical behavior of the platinum-group elements in the mantle, *Geochim. Cosmochim. Acta*, 63, 3915-3934.
- Righter, K., Hauri, E., 1998. Compatibility of Rhenium in garnet during mantle melting and magma genesis, *Science*, 280, 1737-1741.
- Righter, K., Campbell, A. J., Humayun, M., Hervig, R. L., 2004. Partitioning of Ru, Rh, Pd, Re, Ir, and Au between Cr-bearing spinel, olivine, pyroxene and silicate melts, *Geochim. Cosmochim. Acta*, 68, 867-880.
- Roy-Barman, M., Wasserburg, G.J., Papanastassiou, D.A., Chaussidon, M., 1998. Osmium isotopic composition and Re-Os concentrations in sulfide globules from basaltic glasses, *Earth Planet. Sci. Lett.*, 154, 331-347.
- Schilling, J.-G., 1973. Iceland mantle plume, geochemical evidence along Reykjanes Ridge, *Nature*, 242, 565-571.
- Schilling, J.-G., 1991. Fluxes and excess temperatures of mantle plumes inferred from their interaction with migrating mid-ocean ridges, *Nature*, 352, 397-403.
- Schilling, J.-G. Sigurdsson, H., 1979. Thermal minima along the axis of the Mid-Atlantic Ridge, *Nature*, 282, 370-375.
- Schilling, J.-G., Zajac, M., Evans, R., Johnston, T., White, W., Devine, J.D., Kingsley, R., 1983. Petrologic and geochemical variations along the Mid-Atlantic Ridge from 29°N to 73°N, *Amer. J. Sci.*, 283, 510-586.
- Schilling, J.-G., Kingsley, R.H., Fontignie, D., Poreda, R., Xue, S., 1999. Dispersion of the Jan Mayen and Iceland mantle plumes in the Arctic: A He-Pb-Nd-Sr isotope tracer study of basalts from the Kolbeinsey, Mohns, and Knipovich Ridges, *J. Geophys. Res.*, 104, 10543-10569.

- Searle, R. C., Keeton, J. A., Owens, R. B., White, R. S., Mecklenburgh, R., Parsons, B., Lee, S. M., 1998. The Reykjanes Ridge: structure and tectonics of a hot-spot-influenced, slow-spreading ridge, from multibeam bathymetry, gravity and magnetic investigations, *Earth Planet. Sci. Lett.*, 160, 463-478.
- Sigurdsson, H., 1981. First-Order Major Element Variation in Basalt Glasses From the Mid-Atlantic Ridge: 29°N to 73°N, *J. Geophys. Res.*, 86, 9483-9502.
- Skovgaard, A. C., Storey, M., Baker, J., Blusztajn, Hart, J.S.R., 2001. Osmium-oxygen isotopic evidence for a recycled and strongly depleted component in the Iceland mantle plume, *Earth Planet. Sci. Lett.*, 194, 259-275.
- Smallwood, J.R., Staples, R.K., Richardson, R., White, R.S., 1999. Crust generated above the Iceland mantle plume: From continental rift to oceanic spreading center, *Journal of Geophysical Research*, 104, 22,885-22,902.
- Smith, W.H.F., Sandwell, D.T., 1994. Bathymetric prediction from dense satellite altimetry and sparse shipboard bathymetry, *J. Geophys. Res.*, 99, 21803-21824.
- Snow, J. E., Schmidt, G., 1998. Constraints on Earth accretion deduced from noble metals in the oceanic mantle, *Nature*, 391, 166-169.
- Sun, S.-S., Tatsumoto, M., Schilling, J.-G., 1975. Mantle plume mixing along the Reykjanes Ridge axis: Lead isotopic evidence, *Science*, 190, 143-147.
- Tatsumi, Y., Oguri, K., Shimoda, G., 1999. The behaviour of platinum-group elements during magmatic differentiation in Hawaiian tholeiites, *Geochem. J.*, 33, 237-247.
- Tatsumi, Y., Oguri, K., Shimoda, G., Kogiso, T., Barszczus, H.G., 2000. Contrasting behavior of noble-metal elements during magmatic differentiation in basalts from the Cook Islands, Polynesia, *Geology*, 28, 131-134.
- Thirlwall, M. F., Gee, M.A.M., Taylor, R.N., Murton, B. J., 2004. Mantle components in Iceland and adjacent ridges investigated using double-spike Pb isotope ratios, *Geochim. Cosmochim. Acta*, 68, 361-386.
- Turekian, K. K., Clark, S.P., 1969. Inhomogeneous accumulation of the Earth from the primitive solar nebula, *Earth Planet. Sci. Lett.*, 6, 346-348.
- Unni, C. K., 1976. Chlorine and Bromine degassing during submarine and subaerial volcanism. 1976. Ph.D dissertation, Graduate School of Oceanography, University of Rhode Island, 272 pages.
- Unni, C. K., Schilling, J.-G., 1978. Cl and Br degassing by volcanism along the Reykjanes Ridge and Iceland, *Nature*, 272, 19-23.
- Vogel, D C., Keays, R.R., 1997. The petrogenesis and platinum-group element geochemistry the Newer Volcanic Province, Victoria, Australia, *Chemical Geology*, 136, 181-204.
- Vogt, P. R., 1971. Asthenosphere motion recorded by the ocean floor south of Iceland: *Earth Planet. Sci. Lett.* 13, 153-160.
- Wang, Z., Becker, H., 2013. Ratios of S, Se and Te in the silicate Earth require a volatile-rich late veneer, *Nature* 499, 328-331.
- White, R.S., Bown, J.W., Smallwood, J.R., 1995. The temperature of the Iceland plume and origin of outward-propagating V-shaped ridges, *Journal of the Geological Society, London* 152, 1039-1045.
- White, R.S., McBride, J.H., Maguire, P.K.H., Brandsdottir, B., Menke, W., Minshull, T.A., Richardson, K.R., Smallwood, J.R., Staples, R.K., and the FIRE Working Group, 1996.

- Seismic Images of Crust Beneath Iceland Contribute to Long- Standing Debate, *Eos, Trans., Amer. Geophys. Union*, 197, 199-200.
- Wolfe, C.J., Bjarnason, I.T., VanDecar, J.C., Solomon, S.C., 1997. Seismic structure of the Iceland mantle plume, *Nature*, 385, 245-247.
- Woodland, S.J., Pearson, D.G., Thirlwall, M.F., 2002. A platinum Group Element and Re-Os Isotope Investigation of Siderophile Elements Recycling in Subduction Zones: Comparison of Grenada, Lesser Antilles Arc, and the Izu-Bonin Arc, *Journal of Petrology*, 43, 171-198.
- Yang, A.Y., Zhou, M-F., Zhao, T-P., Deng, X-G., Qi, L., Xu, J-F., 2014. Chalcophile elemental compositions of MORBs from ultraslow-spreading Southwest Indian Ridge and controls of the lithospheric structure on S-saturated differentiation. *Chemical Geology*, 382:1-13.

Table 1: PGE contents of basalts from the Reykjanes Ridge and the SWNZ of Iceland, 50-65°N

ID	Group	Lat °N	Lon °W	Depth (m)	(La/Sm) _n	Os (ppb)	Ir (ppb)	Ru (ppb)	Pt (ppb)	Pd (ppb)	Re (ppb)
IC-117g	Iceland	65.00	19.58		0.18	0.300	0.189	0.710	8.42	11.0	1.10
IC19	Iceland	64.66	19.15	-600	0.98	0.010	0.115	0.197	4.54	6.13	0.74
IC11	Iceland	64.27	20.43	-150	1.10	0.026	0.053	0.136	4.62	7.21	0.51
IC12	Iceland	64.28	21.11	-155		0.047	0.052	0.196	4.17	6.19	0.39
IC14	Iceland	64.28	21.11		0.91	0.060	0.168	0.213	12.5	11.8	0.77
IC9	Iceland	64.28	21.11	-146	1.13	0.018	0.042	0.121	4.63	6.12	0.66
IC36	Iceland	64.10	21.90	-250	1.08	0.023	0.169	0.191	5.27	5.93	0.78
IC55	Iceland	63.97	21.74	-30	0.90	0.012	0.024	0.155	2.13	2.57	0.64
IC56	Iceland	63.97	21.74	-80	1.05	0.016	0.047	0.300	2.95	5.39	0.81
IC43	Iceland	63.98	21.97	-300		0.013	0.074	0.094	5.20	6.16	0.66
IC58	Iceland	63.90	22.05	-70	1.25	0.002	0.024	0.050	2.55	2.41	1.09
IC47	Iceland	63.95	22.20	-460	1.25	0.008	0.128	0.080	4.84	5.79	0.76
IC62	Iceland	63.98	22.57	-140	1.17	0.010	0.160	0.064	8.68	9.91	0.94
HS529	Iceland	63.86	22.43	-80	1.25	0.002	0.008	0.012	0.58	0.53	1.55
HS524	Iceland	63.85	22.70	-10	1.14	0.005	0.037	0.043	2.63	3.42	1.24
TR101 15D-8g	T-MORB	63.57	23.70	83	1.01	0.003	0.003	0.016	0.56	0.98	2.00
TR101 19D-1	T-MORB	63.47	23.80	105	1.05	0.016	0.007	0.021	1.11	1.26	1.97
TR101 16D-4	T-MORB	63.47	23.87	60	0.90	0.012	0.015	0.024	1.21	1.39	1.53
TR101 17D-1	T-MORB	63.46	23.85	40	0.94	0.021	0.021	0.024	0.91	1.32	1.23
TR101 18D-1	T-MORB	63.46	23.85	43	1.05	0.015	0.016	0.020	0.83	1.31	2.01
TR101 11D-2g	T-MORB	63.27	24.20	75	1.06	0.007	0.006	0.018	0.36	0.65	1.83
TR101 12D-7g	T-MORB	63.22	24.27	258	1.06	0.002	0.005	0.017	1.92	0.61	2.40
TR101 14D-9g	T-MORB	63.19	24.46	345	0.98	0.003	0.003	0.007	0.36	0.60	2.73
TR101 7D-5g	T-MORB	63.07	24.50	315	0.83	0.004	0.001	0.003	0.21	0.27	2.06
TR101 5D-4g	T-MORB	62.90	24.88	505	1.14	0.017	0.017	0.094	2.75	5.61	2.05
TR101 35D-3g	T-MORB	62.70	25.21	580	0.93	0.014	0.021	0.040	2.02	6.15	2.22
TR101 2D-1g	T-MORB	62.62	25.43	632	0.95	0.011	0.012	0.035	1.68	2.83	2.10
TR101 22D-1g	T-MORB	62.37	25.84	715	0.71	0.011	0.002	0.034	0.36	0.61	2.17
TR101 25D-10g	T-MORB	62.11	26.36	686	0.61	0.008	0.012	0.111	0.49	1.23	2.33
TR101 24D-1g	T-MORB	62.08	26.29	682	0.53	0.015	0.007	0.030	0.57	1.20	2.07
EN025 8D-1g	T-MORB	61.98	26.54	730			0.031	0.543	2.82	8.08	2.68
TR101 27D-7g	T-MORB	61.73	26.88	599	0.54	0.098	0.026	0.210	2.28	5.93	1.70
EN025 6D-1g	T-MORB	61.60	27.07	760	0.66	0.002	0.002	0.016	0.20	0.07	2.42
TR101 29D-4g	T-MORB	61.10	27.88	810	0.40	0.004	0.005	0.014	0.26	0.38	1.87
TR101 30D-10g	T-MORB	61.09	27.90	792	0.31	0.011	0.019	0.120	1.21	1.67	1.84
TR101 33D-6g	T-MORB	60.45	28.88	922	0.16	0.014	0.009	0.043	1.85	2.28	1.71
TR41 D20-3g	N-MORB	60.03	29.38	948	0.27	0.007	0.006	0.021	0.38	0.54	1.82
TR41 D22-1	N-MORB	60.02	29.48	978	0.27	0.027	0.009	0.076	0.86	1.70	1.63
TR41 D19-1g	N-MORB	59.99	29.43	950	0.25	0.019	0.004	0.018	0.50	0.77	1.86
TR41 D38-2g	N-MORB	59.99	29.51	925	0.44	0.009	0.004	0.016	0.38	0.76	1.89
GLJ 10g	N-MORB	58.87	30.95	1383	0.27	0.004	0.002	0.004	0.12	0.10	1.70
EN025 5D-3g	N-MORB	58.42	31.62	1457	0.53	0.011	0.013	0.025	0.88	0.23	1.49
EN025 4D-1g	N-MORB	57.14	33.42	2160	0.42	0.007	0.003	0.040	0.42	0.75	1.55
EN025 3D-4g	N-MORB	55.67	34.87	1975	0.37	0.008	0.006	0.015	0.47	0.24	1.52
EN025 2D-4g	N-MORB	54.76	35.22	2075	0.37	0.004	0.002	0.005	0.20	0.31	2.50
TR100 23D-10g	N-MORB	54.25	35.40	880	0.22		0.005	0.053	0.57	0.71	1.38
EN025 1D-1g	N-MORB	53.41	35.24	2400	0.38	0.003	0.001	0.004	0.07	0.05	1.42
GLJ 7g	N-MORB	52.66	34.94	3239	0.35	0.006	0.003	0.014	0.18	0.16	2.54
TR100 13D-10g	N-MORB	52.48	31.57	4050	0.60	0.004	0.002	0.007	0.14	0.07	0.86
TR138 11D-1g	N-MORB	52.01	29.95	3800	0.52	0.003	0.001	0.002	0.07	0.03	0.91
TR138 9D-2g	N-MORB	51.56	29.92	3710	0.46	0.004	0.003	0.009	0.11	0.06	0.87
TR138 8D-1g	N-MORB	51.28	30.02	3500	0.52	0.002	0.001	0.075	0.06	0.08	0.74
TR138 7D-1Ag	N-MORB	50.46	29.42	3880	0.49	0.006	0.0032	0.0149	2.43	0.25	0.68
Bulk Silicate Earth					1.00	3.40	3.2	5	7.1	3.9	0.28
C1 Chondrites						490	450	710	1010	550	40

Table 1 cont. : Contents of basalts from the Reykjanes Ridge and the SWNZ of Iceland, 50-65°N

ID	Cr (ppm)	Ni (ppm)	Cu (ppm)	Ag (ppb)	Cd (ppb)	SiO ₂ (wt%)	FeOT (wt%)	MgO (wt%)	Mg-Value*
IC-117g	545	235	136	42.2	85.2	47.69	9.46	9.73	68.07
IC19	370	175	118	54.6	78.0	47.40	12.31	9.47	61.46
IC11	296	182	118	31.1	75.0	47.13	11.97	9.23	61.51
IC12				1359	2996	47.46	11.48	10.66	65.81
IC14	354	146	126	50.8	107.6	47.91	11.79	8.19	59.01
IC9	292	127	136	53.1	91.2	47.24	12.08	7.59	56.57
IC36	380	171	144	52.6	89.9	47.51	11.89	9.25	61.72
IC55	261	188	124	20.3	60.6	46.70	12.39	9.11	60.38
IC56	242	110	137	28.7	94.7	47.10	12.94	8.26	56.95
IC43				45.4	70.9	48.35	12.15	8.15	58.17
IC58	163	70	135	42.9	111.0	49.09	13.64	6.90	51.19
IC47	301	111	128	45.6	97.9	48.26	11.74	7.90	58.24
IC62	130	80	127	47.8	77.5	49.20	12.14	7.77	57.02
HS529	95	57	168	49.9	146.1	49.34	14.61	6.19	46.76
HS524	199	89	142	52.7	111.9	49.21	12.32	7.22	54.85
TR101 15D-8g	85	56	132	35.5	139.1				
TR101 19D-1	162	72	137	175.2	135.8	49.69	13.52	6.62	50.37
TR101 16D-4	117	67	118	33.5	115.6	50.19	12.29	7.16	54.70
TR101 17D-1	146	74	102	29.1	100.1	49.67	13.76	6.74	50.38
TR101 18D-1	129	56	131	44.5	133.6	49.84	13.92	6.53	49.30
TR101 11D-2g	109	60	131	33.5	117.5	50.04	14.22	6.42	48.34
TR101 12D-7g	81	60	141	36.3	143.3	50.00	14.08	6.57	49.17
TR101 14D-9g	100	53	120	33.1	144.6				
TR101 7D-5g	89	72	131	34.9	139.6	50.17	12.23	7.79	56.90
TR101 5D-4g	309	100	133	48.1	100.2	50.87	12.16	6.68	53.24
TR101 35D-3g	184	82	109	31.5	140.4	49.81	12.24	7.80	56.91
TR101 2D-1g	243	95	119	37.4	119.8	49.99	12.93	7.05	53.06
TR101 22D-1g	230	86	105	32.2	133.7	50.52	12.1	7.47	56.13
TR101 25D-10g	190	91	98	28.5	131.1				
TR101 24D-1g	224	95	104	28.7	98.0				
EN025 8D-1g				32.8	124.5	51.05	12.49	6.79	52.98
TR101 27D-7g	403	210	113	33.3	111.4	49.60	10.76	8.85	63.02
EN025 6D-1g	74	66	110	31.8	125.4	51.32	12.55	6.98	53.55
TR101 29D-4g	221	91	107	31.1	127.9				
TR101 30D-10g	325	104	112	31.5	127.3	50.04	11.11	8.18	60.41
TR101 33D-6g	242	98	119	33.0	125.5	50.38	11.32	7.89	59.10
TR41 D20-3g	176	134	112	30.1	131.1	49.90	11.59	7.64	57.74
TR41 D22-1	245	106	101	29.9	120.2	51.06	11.50	7.58	57.74
TR41 D19-1g	145	98	107	31.7	103.1	50.16	10.94	8.20	60.84
TR41 D38-2g	159	72	98	29.9	135.4	50.56	11.76	7.16	55.79
GLJ 10g	209	90	91	27.9	119.9	52.12	11.57	7.26	56.53
EN025 5D-3g	377	104	85	29.6	104.2	51.27	10.48	7.71	60.39
EN025 4D-1g	279	116	85	25.3	120.9	50.92	11.28	7.40	57.62
EN025 3D-4g	316	97	95	32.2	107.6				
EN025 2D-4g	278	100	95	26.9	120.0	50.84	11.25	7.48	57.95
TR100 23D-10g	395	154	91	26.0	87.6	49.84	9.93	8.93	65.08
EN025 1D-1g	243	77	75	23.0	117.8	51.09	11.24	7.37	57.61
GLJ 7g	288	122	82	22.7	94.3	51.19	9.90	8.26	63.36
TR100 13D-10g	186	96	68	20.1	133.4	51.86	9.52	7.41	61.74
TR138 11D-1g	221	92	63	20.4	92.4	50.9	9.58	7.81	62.82
TR138 9D-2g	226	86	55	19.6	111.8	51.72	9.65	7.44	61.51
TR138 8D-1g	278	91	50	21.5	105.4	51.84	9.26	8.20	64.73
TR138 7D-1Ag	345	167	62	19.3	81.5	51.63	8.18	8.61	68.57
Bulk Silicate Earth	2625	1960	30	8	40				
C1 Chondrites	2650	10500	120	200	710				

* Based on FeOT and an atomic ratio of $\text{Fe}^{+3}/\text{Fe}^{+3}+\text{Fe}^{+2} = 0.14$

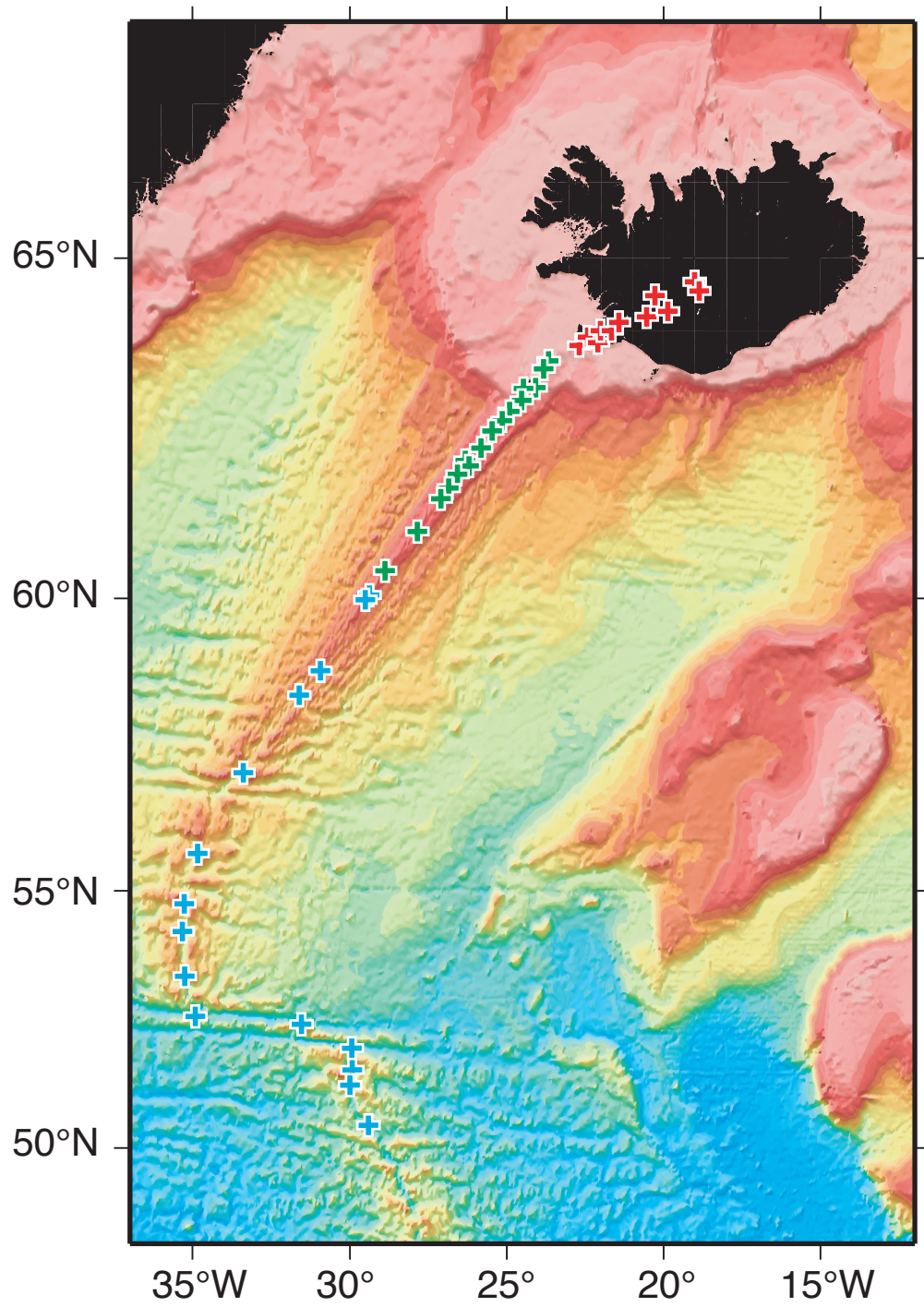


Fig J 1

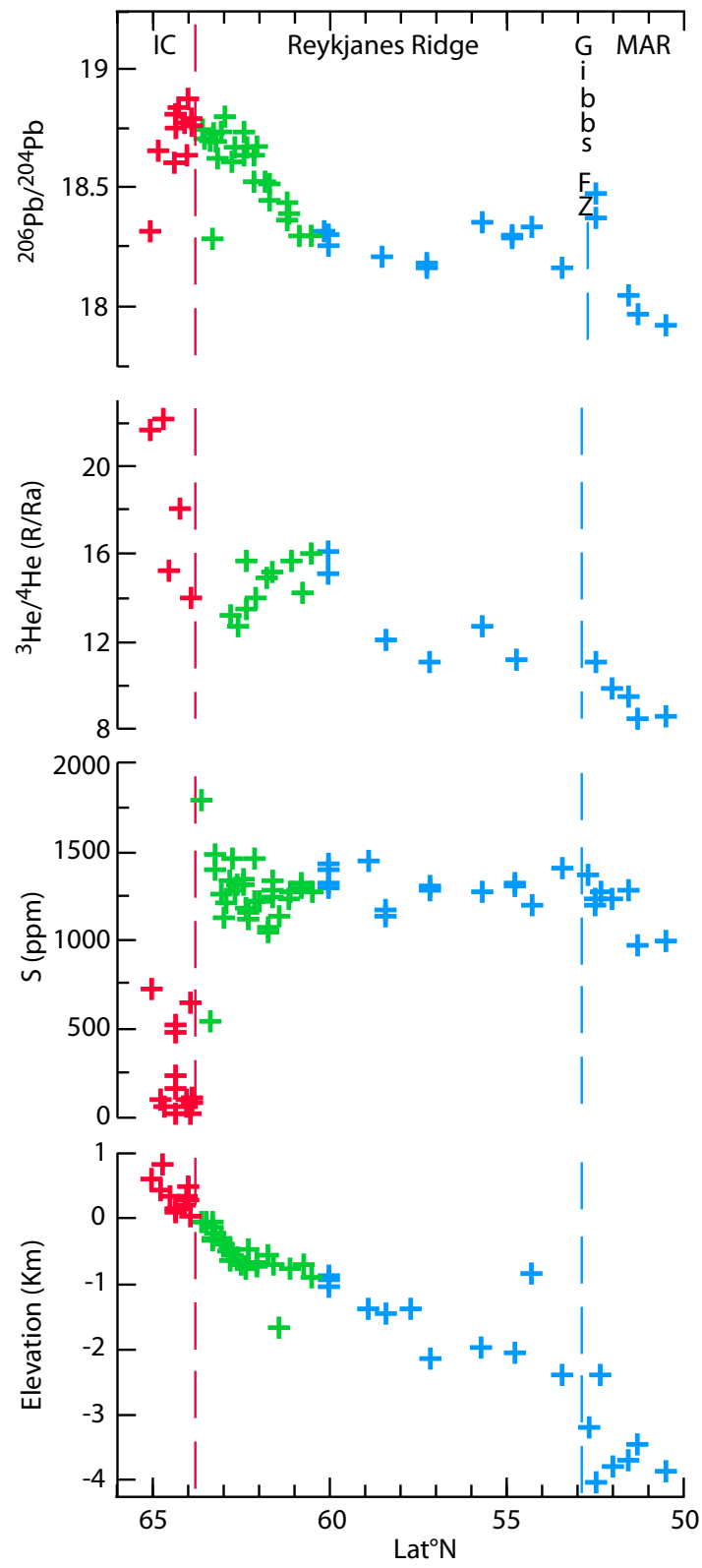


Fig J 2

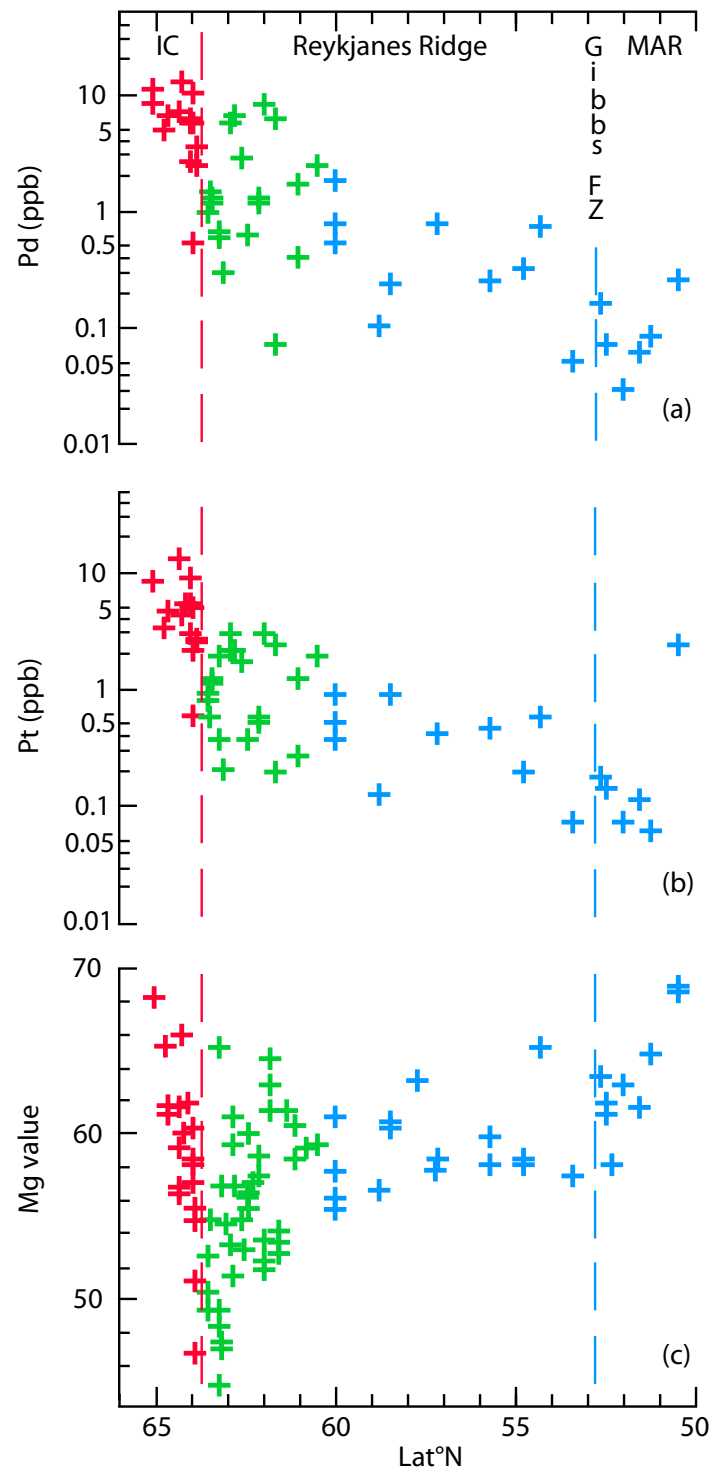


Fig J 3.1

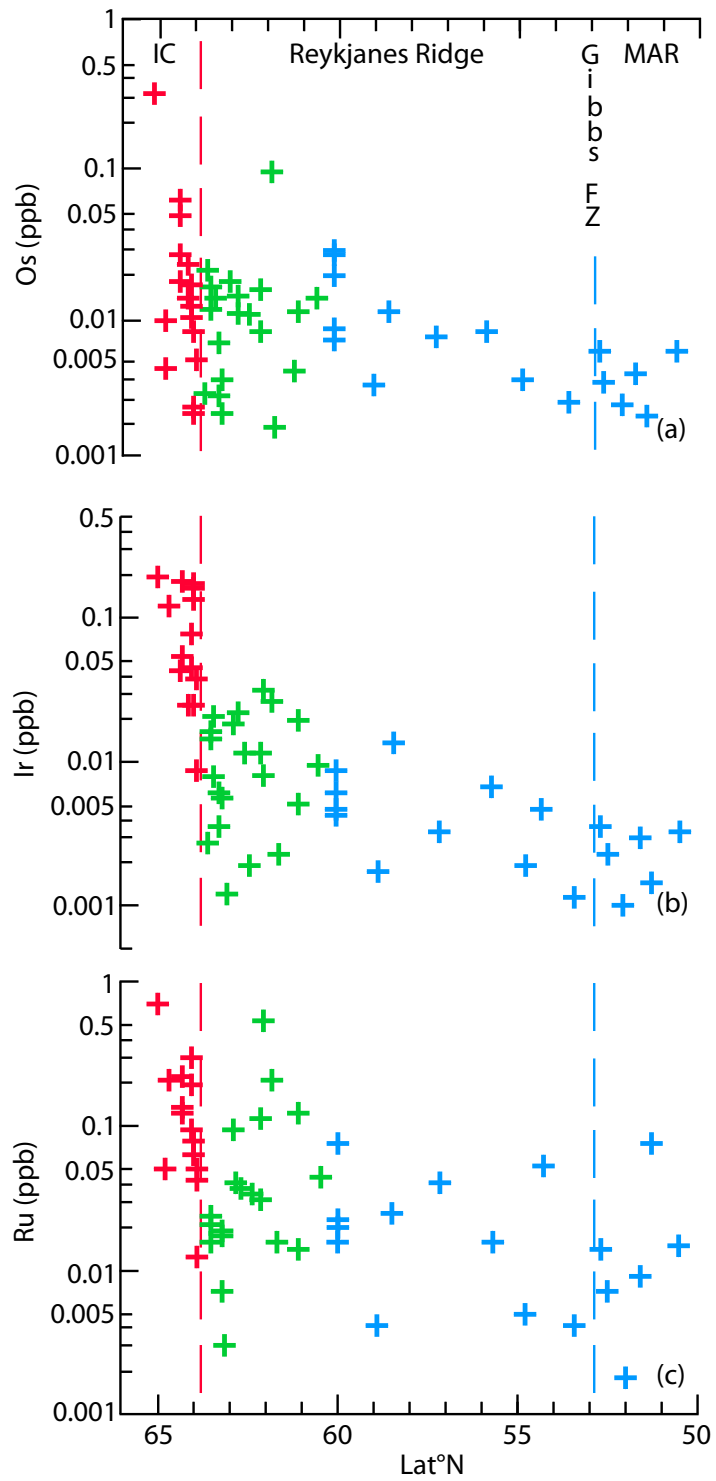


Fig J 3.2

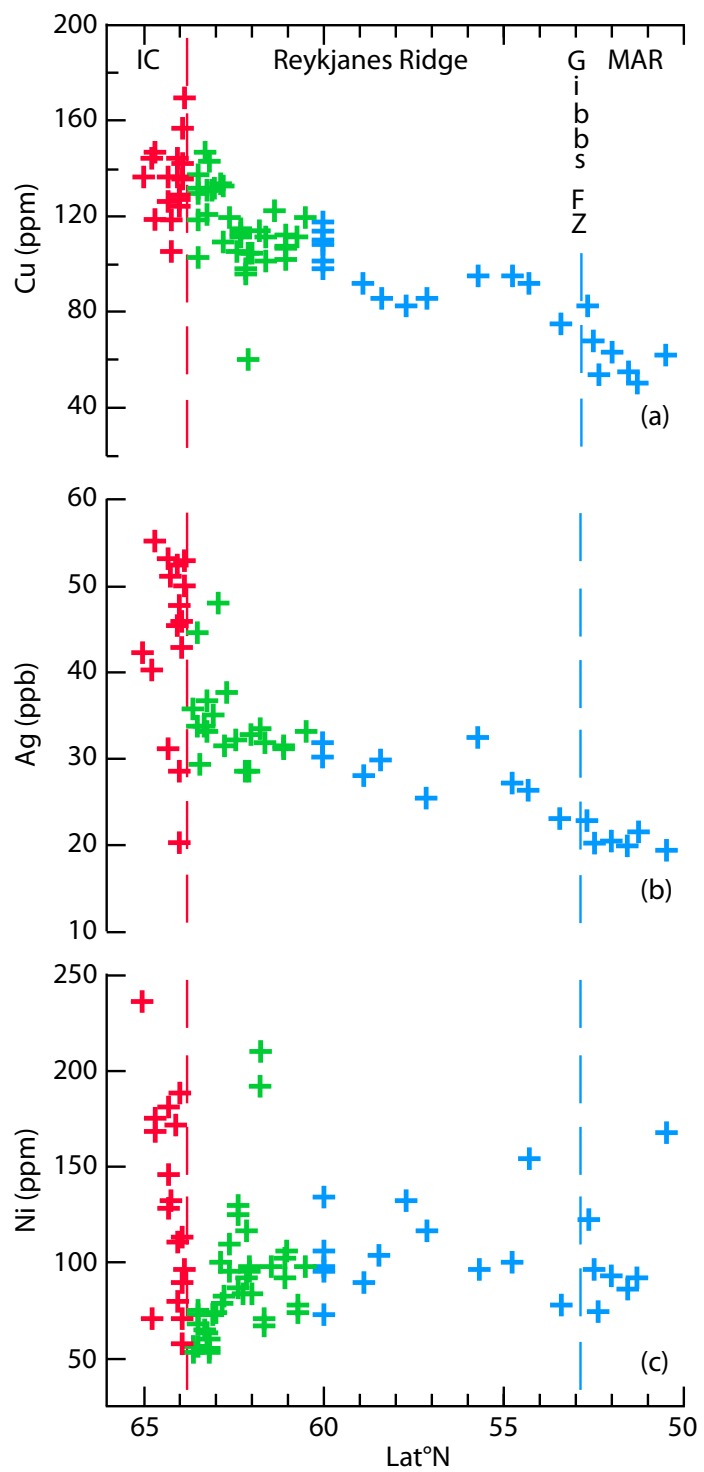


Fig J 3.3

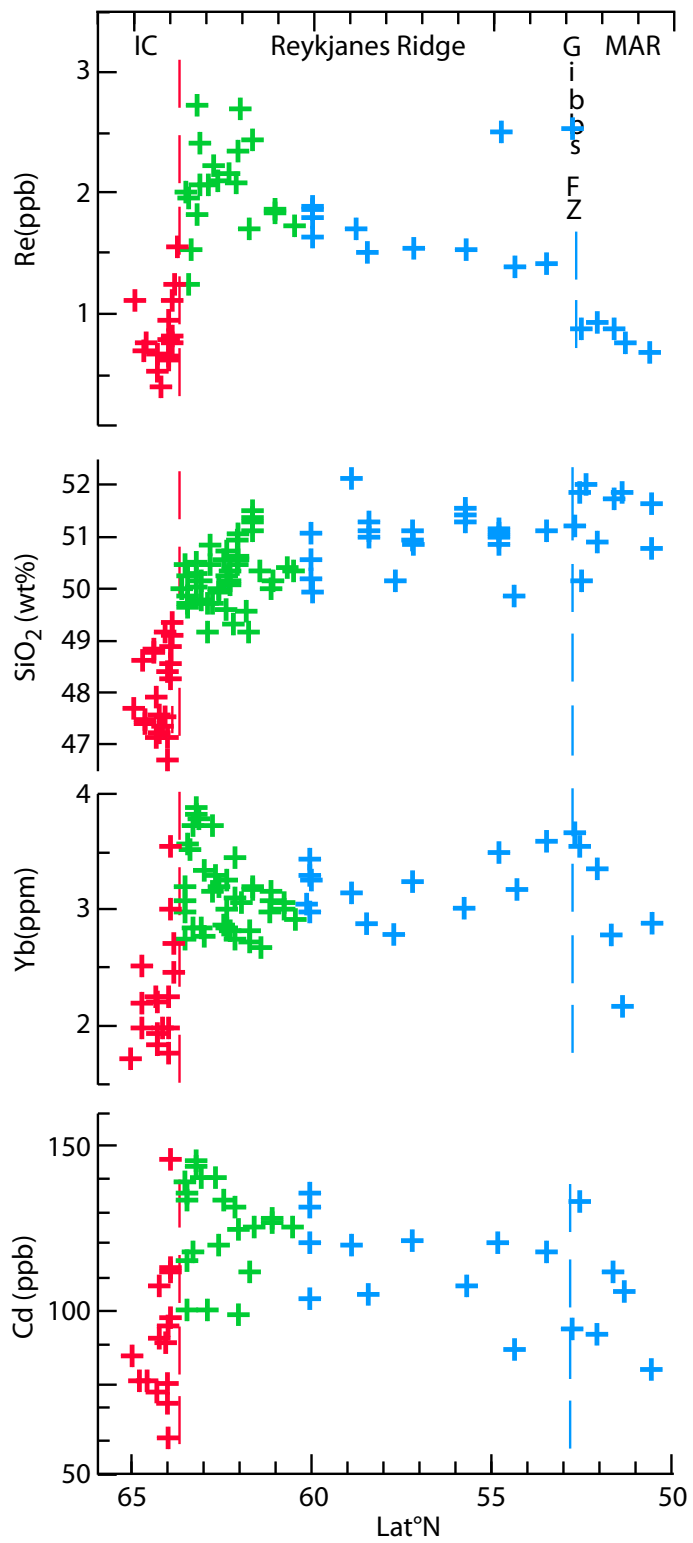


Fig J 4

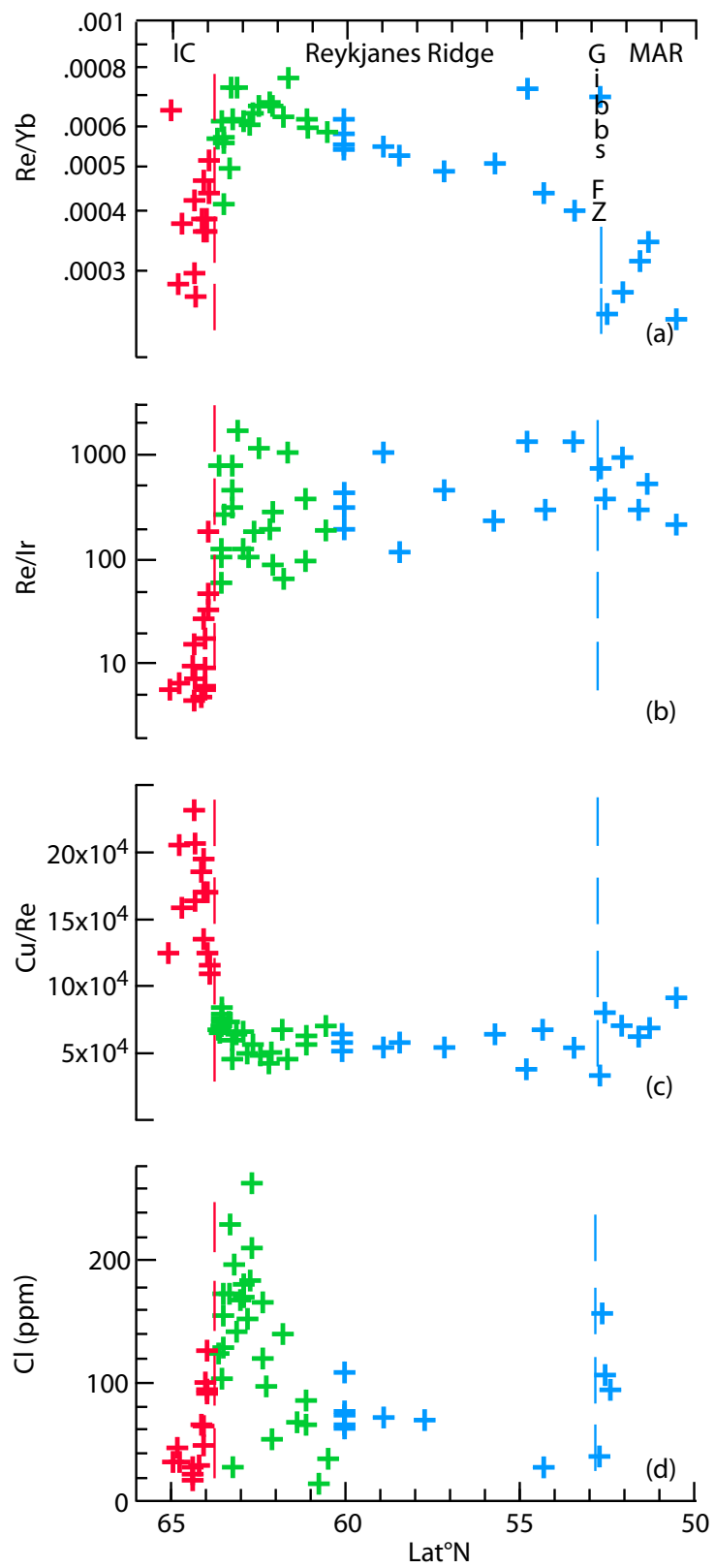


Fig. J 5

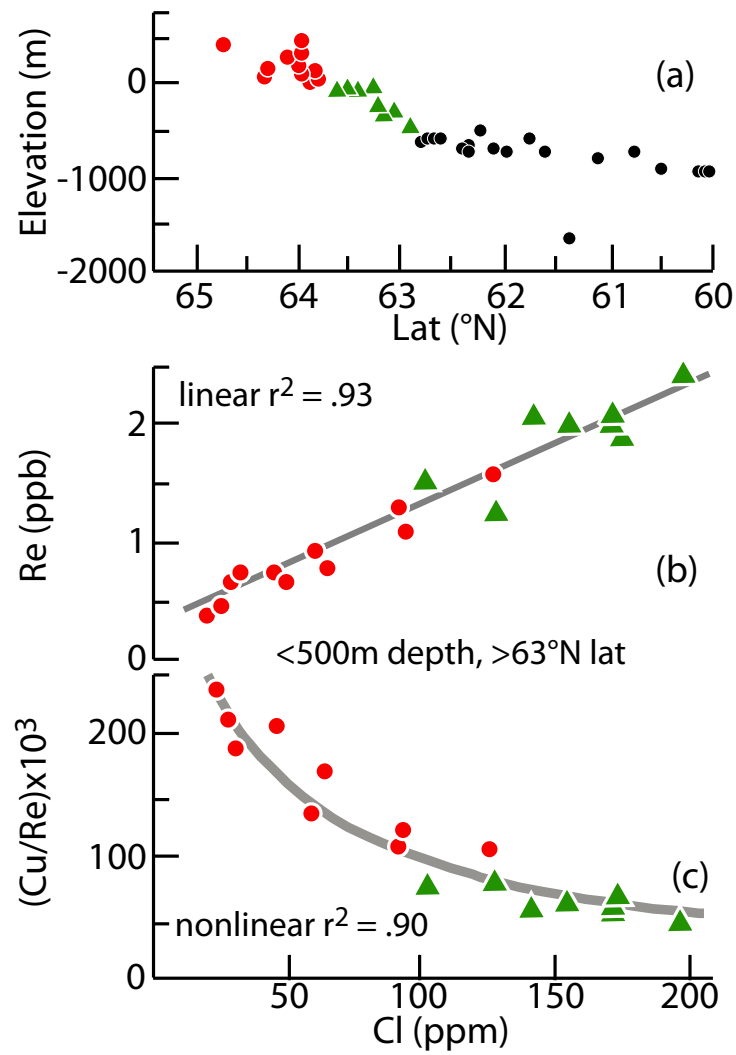


Fig. J 6a-c

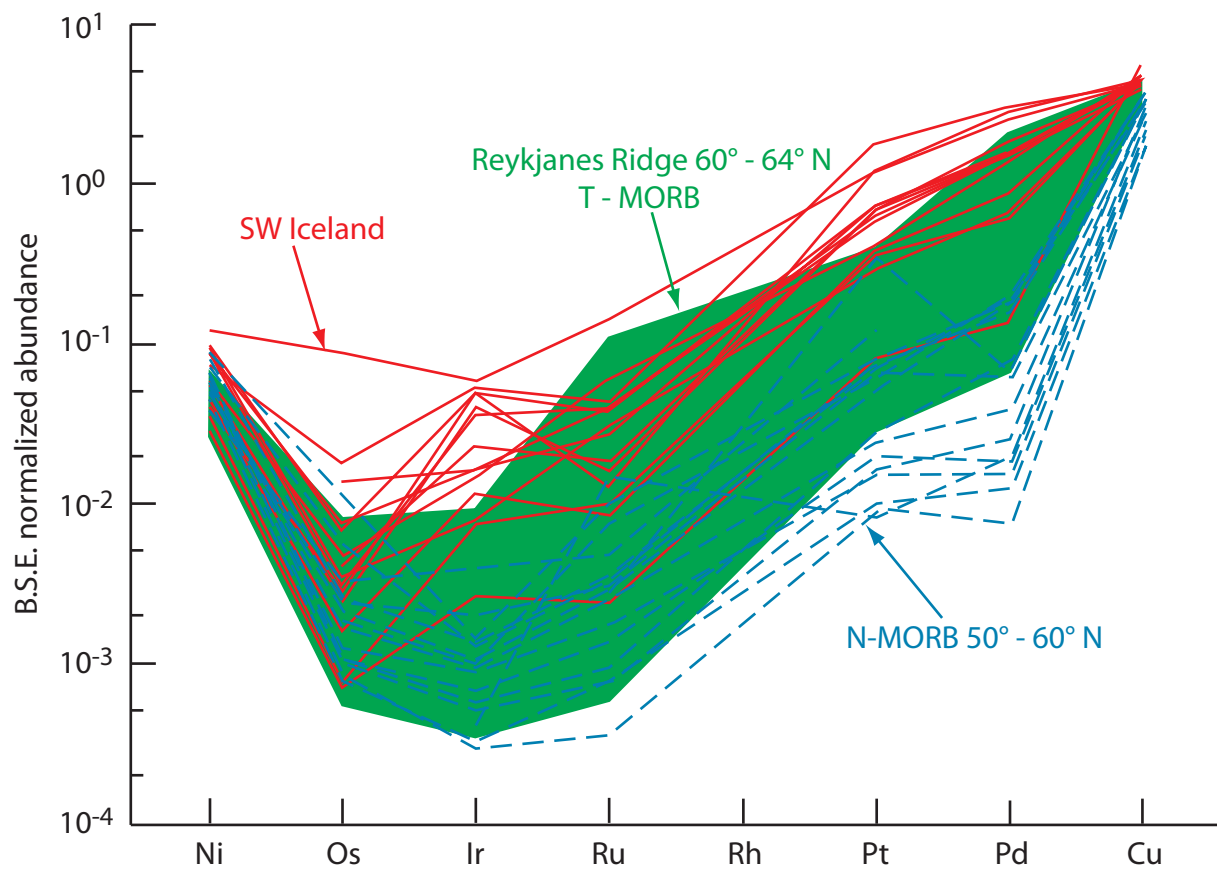


Fig J 7

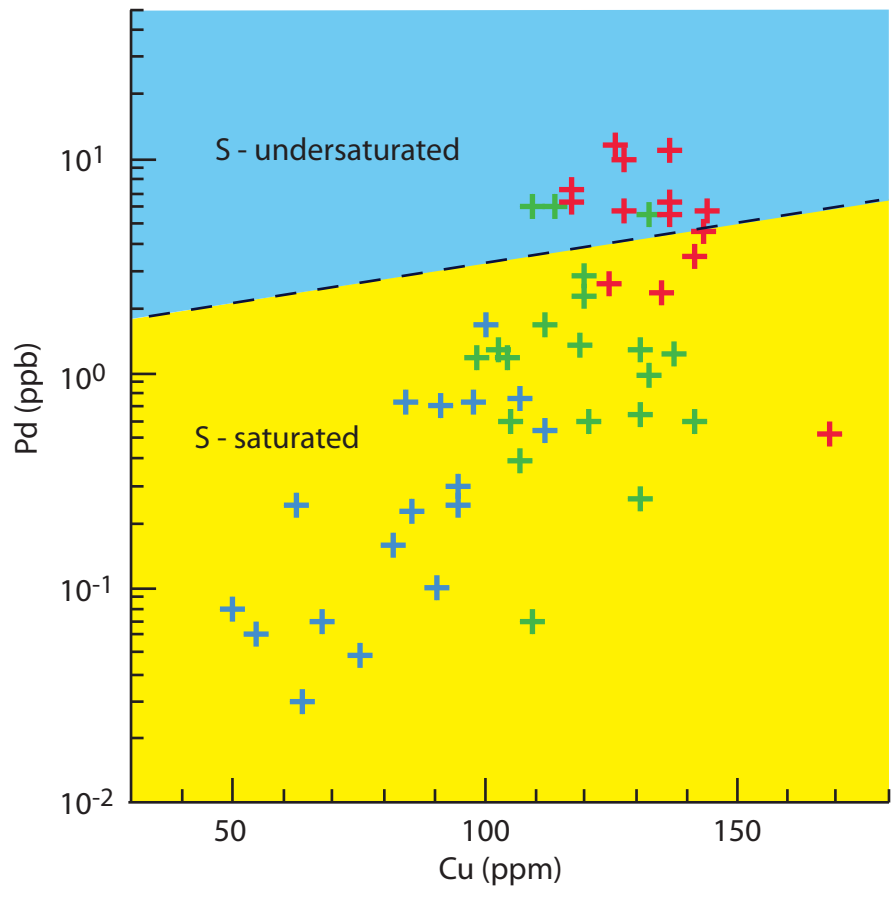


Fig J 8

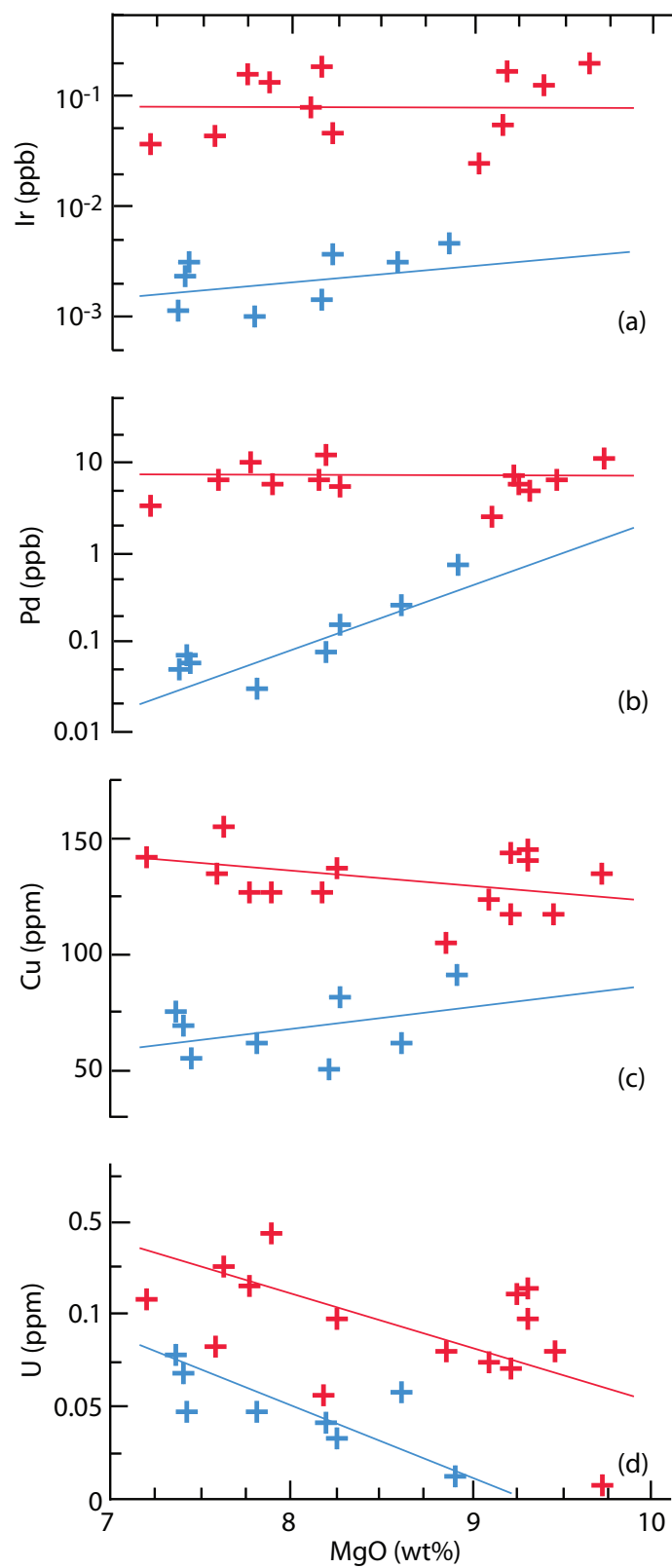


Fig J 9

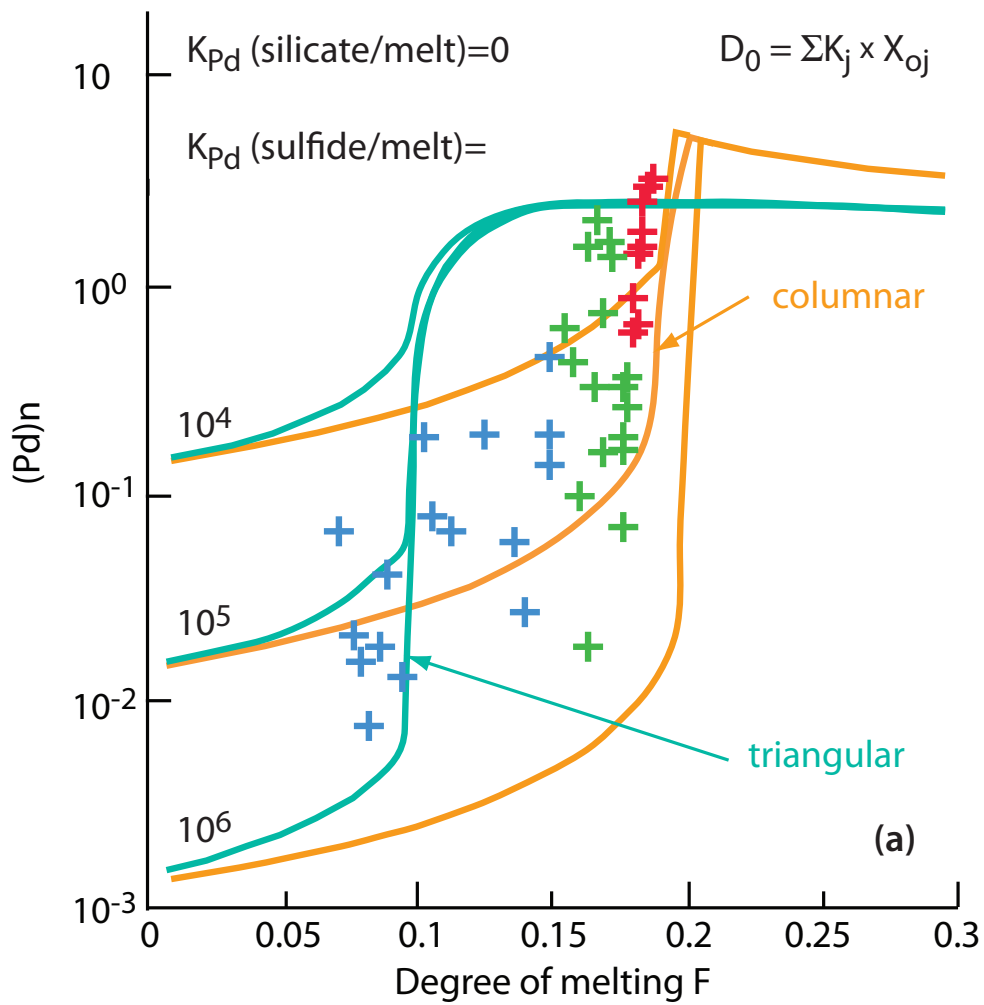


Fig J 10a

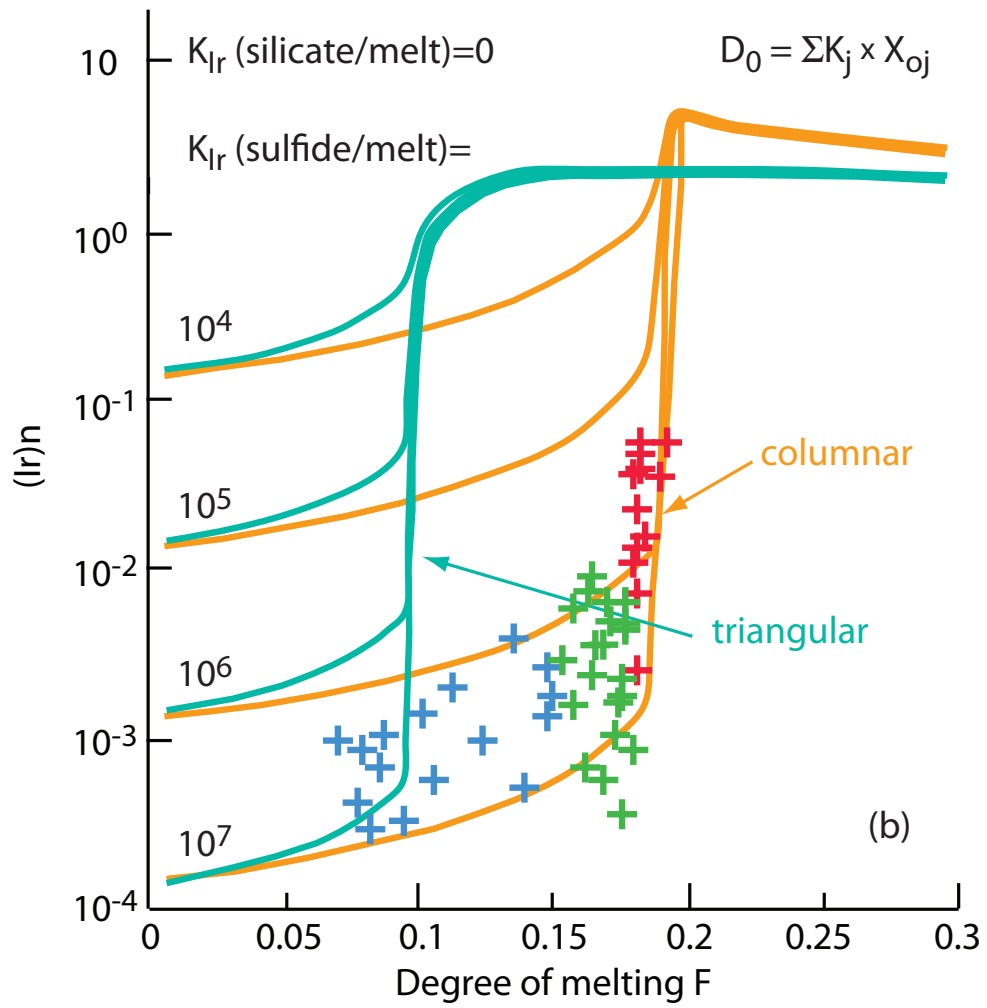


Fig J 10b

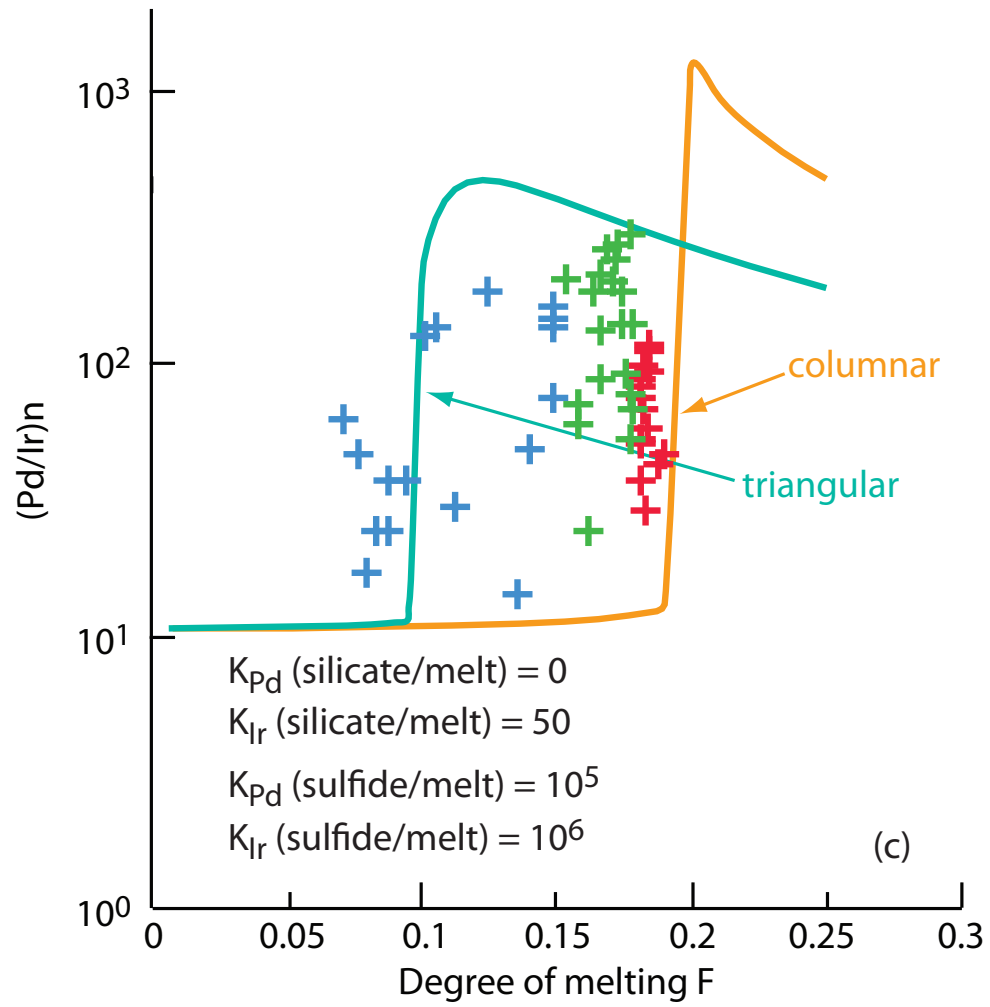


Fig J 10c

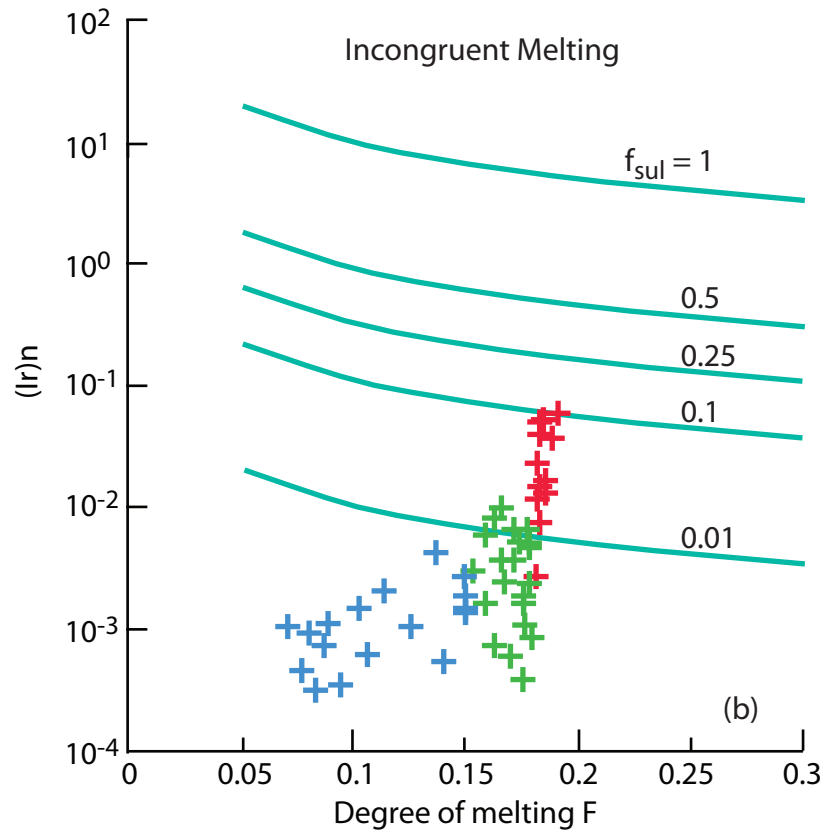


Fig J 11b

Appendix A. Analytical methods, precision and accuracy for analysis of Platinum Group Elements, Rhenium, Cadmium, Silver, Nickel, and Copper in mid-ocean ridge basalts.

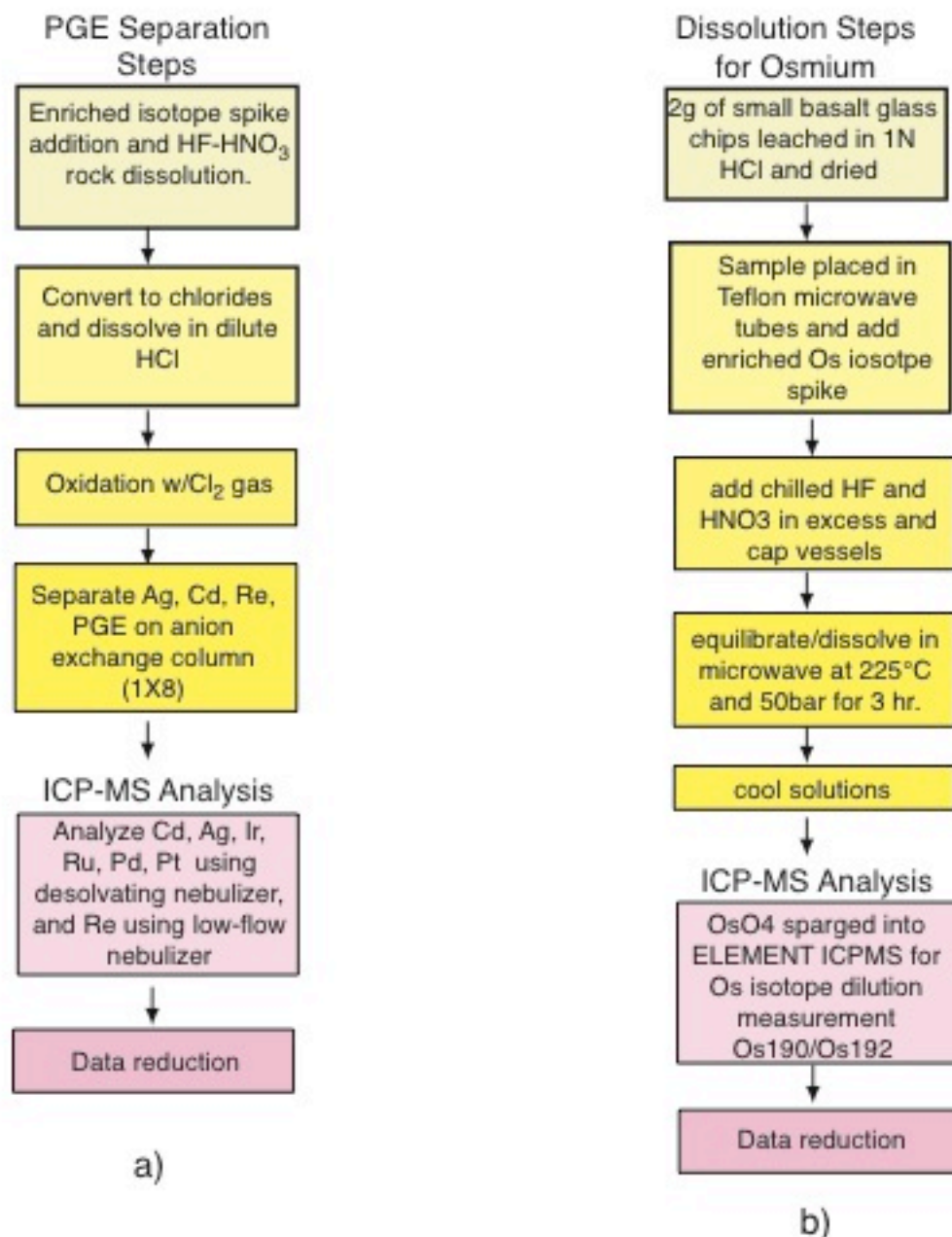


Figure A1. Analytical flow chart for (a) PGE, Re, Ag, Cd, and (b) Os isotopic dilution analysis of basalts and ultramafic rocks. Modified after Pearson and Woodland, 2000, and Hassler et al., 2000.

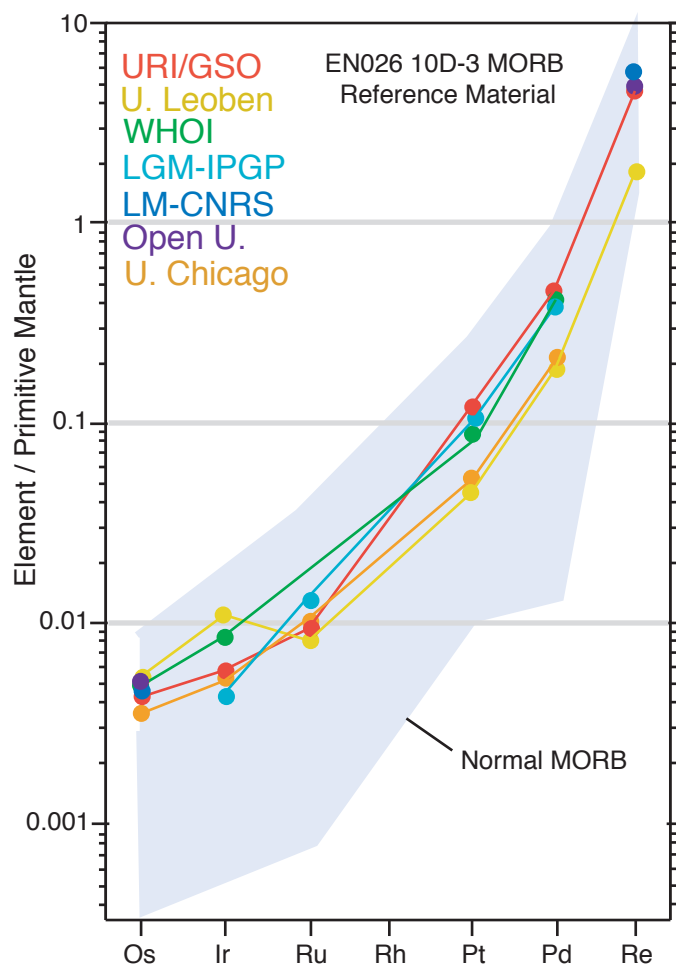


Figure A2: Primitive mantle-normalized PGE and Re patterns obtained for EN026 10D-3 (Mohs Ridge MORB) in the inter-laboratory analyses, and comparison with literature values for normal MORBs (Rehkamper et al., 1999, Kingsley, et al., 2004). Laboratory and investigators were: URI/GSO, Kingsley and Schilling; U. Leoben, Meisel; WHOI, Peucker-Ehrenbrink; LGM-IPGP, Bézoz; LM-CNRS, Escrig; Open U., Gannoun; and U. Chicago, Humayun and Puchtel.

Table A1: Reproducibility in in-house MORB standard EN026 10D-3 for PGE, Re, Cd, and Ag.

dissolution	Os*	Ir	Ru	Pt	Pd	Re	Cd	Ag
1		0.017	0.046	0.85	1.9		115	28
2		0.019	0.046		1.8	1.4	111	25
3		0.017	0.050	0.86	1.9	1.5	115	25
4		0.026	0.052	0.91	1.5	1.1	114	25
5		0.015	0.043	0.77	1.7	1.3	104	28
6		0.015	0.043	0.77	1.7	1.2	104	24
mean (ppb)	0.014	0.018	0.047	0.832	1.8	1.3	111	26
s.d.	0.002	0.0041	0.0037	0.061	0.15	0.16	5.2	1.7
%s.d.	14.7	22.8	7.9	7.3	8.3	12.3	4.7	6.5
Proc. Blank in % of measurement	2.5	0.71	1.3	3.7	0.53	1	0.1	0.03
Proc Blanks in picograms	0.69	0.12	0.62	31	9.3	14	105	9

* Os determined by HF-HNO₃ dissolution in PFA of a microwave oven and sparged into ICPMS; n=19

Table A2: Comparison of inter-laboratory analyses of PGE and Re in EN026 10D-3, MORB standard.

Laboratory	Investigators	Dissolution Method		Os (ppb)	Ir (ppb)	Ru (ppb)	Pt (ppb)	Pd (ppb)	Re (ppb)
URI/GSO	R. Kingsley J-G. Schilling	HF-HNO ₃ PFA (Os microwave/ sparge)	range	.011-.018	.015-.026	.043-.052	.77-.91	1.5-1.9	1.1-1.5
			mean	0.014	0.018	0.047	0.83	1.8	1.3
U. Leoben	T. Meisel	HCL-HNO ₃ HPA-Qz	range	.015-.021	.014-.062	.038-.043	.29-.44	.64-.76	0.47-0.55
			mean	0.018	0.036	0.041	0.37	0.72	0.52
WHOI	B. Peucker- Ehrenbrink	NiS fusion ceramic	range	.014-.020	.023-.029		.52-.72	1.4-1.5	
			mean	0.017	0.027		0.6	1.5	
LGM-IPGP	A. Bezos	HF-HNO ₃ PFA, HCL-HNO ₃ Carius tube	range	.012-.015	.012-.015	.063-.065	.73-.76	1.38-1.57	
			mean	0.014	0.014	0.064	0.75	1.47	
LM-CNRS LGC-IPGP	S. Escrig	HF-HBr PFA	range	.014-.017					1.5-1.7
			mean	0.015					1.6
Open U.	A. Gannoun	HF-HBr PFA	range	.015-.016					1.27-1.28
			mean	0.016					1.28
U. Chicago	M. Humayun I. Puchtel	HCL-HNO ₃ Carius tube	range						
			mean	0.012	0.012	0.017	0.32	0.85	

Table A3: Accuracy of PGE, Re, Cd, and Ag analyses in USGS basalt standards

Element	BIR-1 (picrite)			BHVO-1 (basalt)		
	ppb analyzed	±(%rsd)	Reported*	ppb analyzed	±(%rsd)	Reported*
Ir	0.44	4.3	[0.15]	0.031	14	[0.44]
Ru	0.43	10		0.23	1.4	
Pt	4.9	1.5	[2.8]	4.1	5.2	[2]
Pd	7.1	2.9	[5.6]	3.5	8.3	[3]
Re	0.73	2.3		0.54	24	
Cd	95	1.6	[114]	86	9.7	[69]
Ag	32	2.7	[36]	50	5.6	[55]

*Govindaraju, 1994, brackets indicate reported rather than certified values.

Table A4: Accuracy of Ni and Cu analyses.

Standard	n	Ni (ppm)	Ni %rsd	Cu (ppm)	Cu %rsd
BHVO-1 this study	32	118	2.5	143	4
accepted*		120		136	
BCR-1 this study	30	12	8.5	19	7.7
accepted*		13		19	

*Govindaraju, 1994